RESEARCH ARTICLE | SEPTEMBER 30 2022

Simplicial epidemic model with birth and death

Hui Leng; Yi Zhao ; Jianfeng Luo ; Yong Ye

Chaos 32, 093144 (2022)
https://doi.org/10.1063/5.0092489

Simplicial epidemic model with birth and death

Cite as: Chaos 32, 093144 (2022); doi: 10.1063/5.0092489
Submitted: 23 March 2022 · Accepted: 29 August 2022 ·
Published Online: 30 September 2022

Hui Leng,[1] Yi Zhao,[1,a)] Jianfeng Luo,[1,2,a)] and Yong Ye[1]

AFFILIATIONS

[1]School of Science, Harbin Institute of Technology (Shenzhen), Shenzhen 518055, China
[2]CAS AMSS-PolyU Joint Laboratory of Applied Mathematics (Shenzhen), The Hong Kong Polytechnic University Shenzhen Research Institute, Shenzhen, China

[a)]**Authors to whom correspondence should be addressed:** zhao.yi@hit.edu.cn and gstljf@polyu.edu.hk

ABSTRACT

In this paper, we propose a simplicial susceptible-infected-susceptible (SIS) epidemic model with birth and death to describe epidemic spreading based on group interactions, accompanying with birth and death. The site-based evolutions are formulated by the quenched mean-field probability equations for each site, which is a high-dimensional differential system. To facilitate a theoretical analysis of the influence of system parameters on dynamics, we adopt the mean-field method for our model to reduce the dimension. As a consequence, it suggests that birth and death rates influence the existence and stability of equilibria, as well as the appearance of a bistable state (the coexistence of the stable disease-free and endemic states), which is then confirmed by extensive simulations on empirical and synthetic networks. Furthermore, we find that another type of the bistable state in which a stable periodic outbreak state coexists with a steady disease-free state also emerges when birth and death rates and other parameters satisfy the certain conditions. Finally, we illustrate how the birth and death rates shift the density of infected nodes in the stationary state and the outbreak threshold, which is also verified by sensitivity analysis for the proposed model.

In real propagation, epidemic spread along edge and higher-order structures in networks. The majority of infectious cycles are accompanied with the birth and death of individuals. To capture the complex transmission process with the birth and death, we present a simplicial susceptible-infected-susceptible (SIS) epidemic model with birth and death. Further, the quenched mean-field probability equations of each site in the empty state, the susceptible state and the infected state are derived based on the proposed model. Significantly, extensive simulations on empirical and synthetic structures present that the birth and death rates influence the bistable states (i.e., the coexistence of infection-free and endemic stable states or the coexistence of the stable periodic outbreak state and infection-free state). The explicit effects of birth and death rates on the system can be determined by the mean-field approach. Meanwhile, the outbreak threshold and the density of infected nodes in the stationary state also shift, which is demonstrated by sensitivity analysis of the mean-field system.

I. INTRODUCTION

Research studies on epidemic spread have been focusing on networks' propagation dynamics in recent years.[1–6] A great number of epidemiological research studies on networks have improved our understanding of the mechanism of epidemic spreading.[7–10] In most of the existing research studies, susceptible individuals are infected by their infectious neighbors on the basis of pairwise interactions. Furthermore, on account of group interactions, an individual is also simultaneously exposed to different infectious neighbors, resulting in high-order infection, which is different from pairwise interactions. A fundamentally different mechanism that the infected neighbors transmit to an individual through pairwise and high-order interactions occurs, which results in being unable to be described by complex networks. The occurrence of hypergraph addresses this limitation. De Arruda *et al.* develop a framework that extends the social contagion models when group interactions are introduced and investigate the rich dynamics of social contagion on hypergraphs.[11] Landry and Restrepo establish the hyperdegree-based mean-field equations to describe the dynamics of the SIS model on hypergraphs and study the effect of heterogeneity on hypergraph contagion models.[12] In Ref. 13, a theoretical framework for studying the stability of dynamical systems on an arbitrary hypergraph is given, which is applied to two dynamical processes, i.e., social contagion and diffusion processes.

As one kind of the hypergraph, simplicial complexes contain 1-simplexes (edges), 2-simplexes (triangles) and 3-simplexes

(tetrahedrons), etc., thereby comprehensively describing interactions with various dimensions, which have stimulated the interests of researchers recently. Iacopini *et al.* propose a high-order model of social contagion in which simplicial complexes as underlying structures of networks.[14] They find discontinuous transition and the coexistence region of healthy and endemic states. Matamalas *et al.* conduct the epidemic spreading based on the SIS model in simplicial complexes, which is analytically formulated by the microscopic Markov chain approximation and the epidemic link equations.[15] By the analysis of the fixed point solutions of the model, it is revealed that an abrupt phase transition introducing transmission of 2-simplices emerges. Wang *et al.* propose a simplicial susceptible-infected-recovered-susceptible (SIRS) model to capture the epidemic spreading combining with a nonlinear incidence rate, based on the higher-order structure.[16] It is observed the discontinuous transition and the bistability, as well as the periodic phenomenon of epidemic outbreaks. A new dynamical behavior domain appears in the multi-group simplicial SIS model, where a disease-free equilibrium and an endemic equilibrium coexist and are both locally asymptotically stable.[17] The sufficient conditions of the bistability are obtained. Those research studies show that the dynamical processes on high-order structures bring such abundant dynamical phenomena that exploring them in depth is necessary.

In the above epidemic research studies, the number of individuals is assumed to be constant. In fact, death and birth are natural laws in human evolution, and the death of a human due to a disease may influence the population size, which, in turn, influences the spread of an epidemic. Therefore, it is reasonable to incorporate the birth and death rates into an epidemic model. Liu *et al.* investigate a modified epidemic model with birth and death in regular and scale-free networks.[18] They find that the epidemic threshold is dependent on birth, death, and recovery rates in a regular network, while for uncorrelated networks, the epidemic threshold does not exist in Ref. 18. Further, a study by Zhang *et al.* shows that birth and death rates are related to the epidemic threshold of correlated networks.[19] Birth and death of individuals affect the epidemic threshold as well as the equilibria. In Ref. 20, it is proved that the condition of global asymptotic stability about the endemic equilibrium is in connection with birth and death rates in uncorrelated and correlated networks. Thus, it is important to take the birth and death of humans into account in network epidemic spreading.

Motivated by the above discussions, accompanying birth and death, epidemic spreading based on edge and high-order structures is investigated, described by a simplicial SIS epidemic model with birth and death. Moreover, we derive the quenched mean-field equations of each site and conditions of existence and stability about the system equilibria affected by the birth and death rates. As a consequence of theoretical analysis and numerical simulations on empirical social networks, we find that some system parameters, especially the birth and death rates, influence the existence of a bistable state, which means that in this paper that a disease-free equilibrium coexists with an endemic equilibrium or a periodic oscillation. The density of infected nodes in the stationary state and the outbreak threshold change with the birth and death rates occurring on empirical networks, which are demonstrated by sensitivity analysis of the proposed model.

The paper is organized as follows. In Sec. II, in the context of birth and death of individuals, we introduce high-order interactions in a simplicial SIS epidemic model with birth and death to describe the spreading mechanism. Further, in Sec. III, the spreading evolution is formulated by the quenched mean-field equations of each site and we theoretically analyze the existence and stability of equilibrium. In Sec. IV, numerical simulations on empirical networks with simplex structures are conducted to observe the effect of the birth and death on dynamical behaviors. Sensitivity analysis of the proposed model is conducted to explain the effect of the birth an death rates in Sec. V. We conclude this paper in Sec. VI.

II. SIMPLICIAL SIS EPIDEMIC MODEL WITH BIRTH AND DEATH

We consider that individuals are distributed on the network $\mathscr{G}$ consisting of N sites, in which each site of $\mathscr{G}$ is empty (E) or occupied by an individual being in the susceptible (S) or infected (I) state. At every time step, each site can change its state with a certain probability. An empty site can give birth to a susceptible individual with probability ϕ. In the simplicial SIS epidemic model with birth and death, the channels of disease transmission are pairwise contacts, as well as high-order interactions, which are modeled by simplicial complexes. A k-simplex δ_k is a set of $k+1$ vertices, denoted by $\delta_k = [v_0, \ldots, v_k]$, where k is the dimension of simplex δ_k. Any subset $\delta_{k'}(k' \leq k)$ of δ_k is its subsimplex, which is called face of simplex δ_k in algebraic topology. Normally, a simplicial complex K on a given set of vertices V, with $|V| = N$, is a collection of simplices such that if simplex δ_k is in K, and τ_p is a face of δ_k, then τ_p is in K; and if two simplices δ_n and τ_r are in K, then $\delta_n \cap \tau_r$ is either empty or is a common face of δ_n and τ_r. We call nodes (or vertices) the

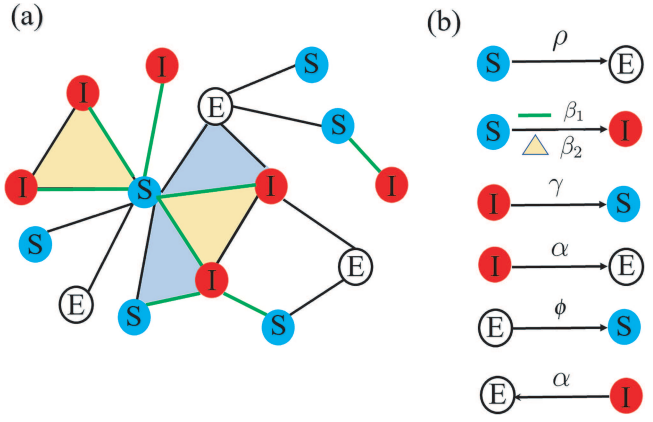

FIG. 1. (a) A network with 15 sites, where white sites are empty, and blue and red sites are occupied by the susceptible and infected individuals, respectively. (b) The state-transition rules of a site. The left and right side of the arrow represent the current state of a site and the state after the change, respectively, and the letter on the arrow denotes the state change rate, where epidemic spreadings through 1-simplex (green edge) and 2-simplex (yellow triangle) with rates β_1 and β_2, respectively.

0-simplex and links (or edges) the 1-simplex of a simplicial complex K, and 2-simplex corresponds to the triangles, 3-simplex to the tetrahedra of K, and so on, so as to be consistent with the standard network nomenclature. In unit time, a susceptible individual can be infected with probability $\beta_1, \beta_2, \beta_3, \ldots, \beta_k$ through 1-simplex, 2-simplex, 3-simplex, …, k-simplex. Here, it is assumed that the residual individuals except the susceptible individual in 2-simplex, 3-simplex, …, k-simplex are all in the infected state. And a susceptible individual dies with probability ρ. An infected individual can recover from a disease with probability γ and die with probability α due to the disease. If an individual dies, there is an empty site left. It is obvious that if $\beta_2, \beta_3, \ldots, \beta_k, \phi, \rho$ and α equal 0, the model becomes an SIS model; and if $\beta_2, \beta_3, \ldots, \beta_k$, ϕ, γ and α equal 0, the model reduces to an susceptible-infected-recovered (SIR) model.

Take a network with 15 sites as an example, as shown in Fig. 1(a). There are three empty sites, and the remaining sites are equally occupied by susceptible and infected individuals, which are labeled as E, S, and I, respectively. The network contains 19 1-simplex (green and black edges) and 4 2-simplex (yellow and blue triangles), where epidemic spreadings through 1-simplex (green edge) and 2-simplex (yellow triangle) with rates β_1 and β_2, respectively. Any site may change its state at each time step, and the state-transition rules are shown in Fig. 1(b).

III. THE QUENCHED MEAN-FIELD EVOLUTION ON A SIMPLICIAL SIS EPIDEMIC MODEL WITH BIRTH AND DEATH

In order to figure out how the disease evolves over time, the mathematical expression of the above propagation process is particularly significant. In this paper, we take advantage of the quenched mean-field method to obtain the state evolution equation of each site.

Let $E_i(t)$, $S_i(t)$, and $I_i(t)$ be the probability that site i is in the empty state, the susceptible state and the infected state at time t, respectively. According to the state-transition rules of site i, at time t the birth on site i causes the decrease of $E_i(t)$ and increase of $S_i(t)$, while the death of individual i leads to the increase of $E_i(t)$ and decrease of $S_i(t)$ and $I_i(t)$. A susceptible individual i is infected through the simplex at time t, resulting in the increase of $I_i(t)$ and decrease of $S_i(t)$. Therefore, the dynamical equations for $E_i(t)$, $S_i(t)$, and $I_i(t)$ are denoted by

$$\begin{aligned}
\frac{dE_i(t)}{dt} &= -\phi E_i(t) + \rho S_i(t) + \alpha I_i(t),\\
\frac{dS_i(t)}{dt} &= \phi E_i(t) + \gamma I_i(t) - \rho S_i(t)\\
&\quad - S_i(t)\sum_{m=1}^{d^i}\beta_m \sum_{\delta_m\in\mathscr{A}_m^i}\prod_{j_z\in\delta_m, z=1}^{m} I_{j_z}(t),\\
\frac{dI_i(t)}{dt} &= -\gamma I_i(t) - \alpha I_i(t) + S_i(t)\sum_{m=1}^{d^i}\beta_m \sum_{\delta_m\in\mathscr{A}_m^i}\prod_{j_z\in\delta_m, z=1}^{m} I_{j_z}(t),
\end{aligned} \tag{1}$$

where d^i denotes the maximal dimension of the simplex to which site i belongs. $\mathscr{A}_m^i$ is the set of simplices of dimension m in all simplices to which site i belongs. $S_i(t)\beta_m \sum_{\delta_m\in\mathscr{A}_m^i}\prod_{j_z\in\delta_m, z=1}^{m} I_{j_z}(t)$ is the probability that the susceptible individual i is infected through m-simplex. All m-simplices which individual i belongs to should be taken into account since the probability evolution is calculated here. In addition, individual i can be infected through its associated simplices, thereby considering dimensions of simplices from $m = 1$ to d^i.

In the spreading through simplices, we assume that all the other individuals except the susceptible individual i are in the infected state at the same time, which is a small probability event, especially in high-dimension simplices.[14,16] Thus, here, we just consider simplices of dimension up to 2 and take all the possible pairwise interactions (1-simplex) and triangular interactions (2-simplex) into account. The dynamical equations are then given as

$$\begin{aligned}
\frac{dE_i(t)}{dt} &= -\phi E_i(t) + \rho S_i(t) + \alpha I_i(t),\\
\frac{dS_i(t)}{dt} &= \phi E_i(t) + \gamma I_i(t) - \rho S_i(t) - \beta_1 S_i(t)\sum_{j\in\mathscr{N}_i} I_j(t) - \beta_2 S_i(t)\\
&\quad \times \sum_{\delta_2=\{j_1,j_2\}\in\mathscr{A}_2^i} I_{j_1}(t) I_{j_2}(t),\\
\frac{dI_i(t)}{dt} &= -\gamma I_i(t) - \alpha I_i(t) + \beta_1 S_i(t)\sum_{j\in\mathscr{N}_i} I_j(t) + \beta_2 S_i(t)\\
&\quad \times \sum_{\delta_2=\{j_1,j_2\}\in\mathscr{A}_2^i} I_{j_1}(t) I_{j_2}(t),
\end{aligned} \tag{2}$$

where $\mathscr{N}_i$ is the set of the neighbors of site i. $\mathscr{A}_2^i$ denotes the set of 2-simplices to which site i belongs. $\beta_1 S_i(t)\sum_{j\in\mathscr{N}_i} I_j(t)$ and $\beta_2 S_i(t)\sum_{\delta_2=\{j_1,j_2\}\in\mathscr{A}_2^i} I_{j_1}(t) I_{j_2}(t)$ represent the probability of getting infected through 1-simplices and 2-simplices for the susceptible individual i, respectively.

In general, only a few nodes are in the infected state at the initial period of epidemic spreading, i.e., $I_i(0) \to 0$. Hence, we linearize $\frac{dI_i(t)}{dt}$ in Eq. (2) around $I_i(0) \to 0$, whose matrix form can be written as

$$\frac{d\mathscr{I}(t)}{dt} = \left[-(\gamma+\alpha)\mathbb{I}_N + \beta_1\frac{\phi}{\phi+\rho}\mathscr{A}\right]\mathscr{I}(t), \tag{3}$$

where $\mathscr{I}(t) = (I_1(t), I_2(t), \ldots, I_N(t))^T$, and $\mathbb{I}_N$ is a N dimensional identity matrix. $\mathscr{A}$ is the adjacency matrix of the network. When the maximum eigenvalue of matrix $(-(\gamma+\alpha)\mathbb{I}_N + \beta_1\frac{\phi}{\phi+\rho}\mathscr{A})$ is greater than 0, the disease breaks out. Hence, we obtain the epidemic threshold

$$\beta_1^{c(net)} = \frac{(\gamma+\alpha)(\phi+\rho)}{\phi\bigwedge_{\mathscr{A}}},$$

where $\bigwedge_{\mathscr{A}}$ is the maximum eigenvalue of matrix $\mathscr{A}$. Obviously, the birth, death, recovery rates, and the network topology have an effect on the epidemic threshold.

Equation (2) gives the probability evolution of site i in each state, thereby obtaining evolution equations of all sites. The dimension of differential equations for a whole network is high since the number of sites in the network is large, which makes it difficult to

analyze dynamic behaviors. Under a homogeneous mixing hypothesis, we introduce the mean-field (MF) approach to reduce the dimension, thereby obtaining the existence and stability conditions of equilibria. Let $E(t)$, $S(t)$, and $I(t)$ be the density of empty sites, susceptible individuals, and infected individuals at time t, respectively. According to Eq. (2), the MF expressions of the time evolution are written as

$$\begin{aligned}\frac{dE(t)}{dt} &= -\phi E(t) + \alpha I(t) + \rho S(t),\\ \frac{dS(t)}{dt} &= \phi E(t) + \gamma I(t) - \rho S(t) - \beta_1\langle k_1\rangle S(t)I(t) - \beta_2\langle k_2\rangle S(t)I^2(t),\\ \frac{dI(t)}{dt} &= -\gamma I(t) - \alpha I(t) + \beta_1\langle k_1\rangle S(t)I(t) + \beta_2\langle k_2\rangle S(t)I^2(t).\end{aligned} \tag{4}$$

Since the definitions of $E(t)$, $S(t)$, and $I(t)$ naturally fulfill the condition $E(t) + S(t) + I(t) = 1$, system (4) can be reduced to a two-dimensional differential system

$$\begin{aligned}\frac{dE(t)}{dt} &= -(\phi+\rho)E(t) + (\alpha-\rho)I(t) + \rho,\\ \frac{dI(t)}{dt} &= (\beta_1\langle k_1\rangle - \gamma - \alpha)I(t) - \beta_1\langle k_1\rangle E(t)I(t) - \beta_2\langle k_2\rangle E(t)I^2(t)\\ &\quad + (\beta_2\langle k_2\rangle - \beta_1\langle k_1\rangle)I^2(t) - \beta_2\langle k_2\rangle I^3(t).\end{aligned} \tag{5}$$

Then, we analyze the existence and stability of equilibria in system (5), which is discussed in detail in the Appendix. We set $F_1 = (E_1, I_1)$, $F_2 = (E_2, I_2)$, where $E_1 = \frac{(\alpha-\rho)I_1+\rho}{(\phi+\rho)}$, $E_2 = \frac{(\alpha-\rho)I_2+\rho}{(\phi+\rho)}$, $I_1 = \frac{(\phi+\alpha)\beta_1\langle k_1\rangle(R_1-1)+\sqrt{\Delta_1}}{2(\phi+\alpha)\beta_2\langle k_2\rangle}$, $I_2 = \frac{(\phi+\alpha)\beta_1\langle k_1\rangle(R_1-1)-\sqrt{\Delta_1}}{2(\phi+\alpha)\beta_2\langle k_2\rangle}$, $R_1 = \frac{\phi\beta_2\langle k_2\rangle}{(\phi+\alpha)\beta_1\langle k_1\rangle}$ $\Delta_1 = ((\phi+\alpha)\beta_1\langle k_1\rangle(R_1-1))^2 - 4\phi(\alpha+\phi)\beta_1\beta_2\langle k_1\rangle\langle k_2\rangle(1-R_0)/R_0$ and $R_0 = \frac{\phi\beta_1\langle k_1\rangle}{(\gamma+\alpha)(\phi+\rho)}$. We obtain the following theorem. The theorem proof is given in the Appendix.

Theorem 1. (1) *System (5) has a unique disease-free equilibrium* $F_0 = \left(\frac{\rho}{\phi+\rho}, 0\right)$.

(2) *If* $\alpha > \rho$, *system (5) has a unique endemic equilibrium* F_1 *when* $R_0 > 1$, *and two endemic equilibria* F_1 *and* F_2 *when* $R_1^* \le R_0 < 1$ *and* $1 < R_1 < \min\left\{\frac{2\beta_2\langle k_2\rangle}{\beta_1\langle k_1\rangle} + 1, \frac{2\phi\beta_2\langle k_2\rangle}{(\alpha-\rho)\beta_1\langle k_1\rangle} + 1\right\}$.

(3) *If* $\alpha < \rho$, *system (5) has a unique endemic equilibrium* F_1 *when* $R_0 > 1$, *and two endemic equilibria* F_1 *and* F_2 *when* $R_1^* \le R_0 < 1$ *and* $1 < R_1 < \frac{2\beta_2\langle k_2\rangle}{\beta_1\langle k_1\rangle} + 1$.

In addition, let $R_0 = 1$, and we derive the epidemic outbreaks threshold of system (5), which is

$$\beta_1^c = \frac{(\gamma+\alpha)(\phi+\rho)}{\phi\langle k_1\rangle}. \tag{6}$$

Once $\Delta_1 > 0$, $f(x) = 0$ admits two different roots I_1 and I_2, which implies that the bistable state may occur. When $\Delta_1 = 0$, $f(I) = 0$ admits two identical roots, i.e., $I_1 = I_2$. And then, we derive another epidemic threshold β_1^0 from $\Delta_1 = 0$,

$$\beta_1^0 = \max\left\{\frac{\sqrt{4(\phi+\alpha)(\gamma+\alpha)(\phi+\rho)\beta_2\langle k_2\rangle} - \phi\beta_2\langle k_2\rangle}{(\phi+\alpha)\langle k_1\rangle}, 0\right\}, \tag{7}$$

called as the minimum infectivity parameter. When $0 < \beta_1 < \beta_1^0$, there is only a disease-free equilibrium of system (5); When $\beta_1^0 < \beta_1 < \beta_1^c$, system (5) must have a disease-free equilibrium, and two endemic equilibria under some conditions; when $\beta_1 > \beta_1^c$, there exists a endemic equilibrium only.

Theorem 2. *The disease-free equilibrium* F_0 *is locally asymptotically stable if* $\beta_1 < \beta_1^c$, *and unstable if* $\beta_1 > \beta_1^c$.

Denote

$$\begin{aligned}\Delta_2 &= \left(\frac{2\phi}{(\phi+\rho)}\beta_2\langle k_2\rangle - \frac{(\alpha+2\phi+\rho)}{(\phi+\rho)}\beta_1\langle k_1\rangle\right)^2\\ &\quad - \frac{4\phi(3\phi+2\alpha+\rho)\beta_1\beta_2\langle k_1\rangle\langle k_2\rangle}{(\phi+\rho)^2}(1-R_2)/R_2,\\ z_1 &= \frac{2\phi\beta_2\langle k_2\rangle - (\alpha+2\phi+\rho)\beta_1\langle k_1\rangle + (\phi+\rho)\sqrt{\Delta_2}}{2(2\alpha+3\phi+\rho)\beta_2\langle k_2\rangle}\end{aligned}$$

and

$$z_2 = \frac{2\phi\beta_2\langle k_2\rangle - (\alpha+2\phi+\rho)\beta_1\langle k_1\rangle - (\phi+\rho)\sqrt{\Delta_2}}{2(2\alpha+3\phi+\rho)\beta_2\langle k_2\rangle}.$$

Theorem 3. (1) *If* $\Delta_2 < 0$, *the endemic equilibrium* F_1 *is locally asymptotically stable.*

(2) *If* $\Delta_2 > 0$, $\frac{2\phi\beta_2\langle k_2\rangle}{(\alpha+2\phi+\rho)\langle k_1\rangle} < \beta_1 < \frac{(\phi+\rho)(\alpha+\gamma+\phi+\rho)}{\phi\langle k_1\rangle}$ *and* $\beta_2 < \frac{(\phi+\rho)(\alpha+2\phi+\rho)(\alpha+\gamma+\phi+\rho)}{2\phi^2\langle k_2\rangle}$, *the endemic equilibrium* F_1 *is locally asymptotically stable.*

(3) *If* $\Delta_2 > 0$ *and* $\beta_1 > \frac{(\phi+\rho)(\alpha+\gamma+\phi+\rho)}{\phi\langle k_1\rangle}$, *the endemic equilibrium* F_1 *is locally asymptotically stable when* $I_1 \in (z_1, 1]$.

(4) *If* $\Delta_2 > 0$ *and* $\beta_1 < \min\left\{\frac{(\phi+\rho)(\alpha+\gamma+\phi+\rho)}{\phi\langle k_1\rangle}, \frac{2\phi\beta_2\langle k_2\rangle}{(\alpha+2\phi+\rho)\langle k_1\rangle}\right\}$, *the endemic equilibrium* F_1 *is locally asymptotically stable when* $I_1 \in (0, z_2) \cup (z_1, 1]$.

(5) *The endemic equilibrium* F_2 *is a saddle.*

A. Numerical examples

Based on the above analysis of equilibria and their stability, we further verify these findings by numerical simulations.

In terms of the existence conditions of equilibria, the forward and backward bifurcations separately exist for system (5) under different birth rates ϕ. As shown in Fig. 2(a), when $\phi = 0.2$ and other parameters are fixed, the backward bifurcation (the red curve) appears, thereby arising the bistable state. In this case, we derive two threshold $\beta_1^c = 0.2125$ and $\beta_1^0 = 0.12$, which are marked in Fig. 2(a). When $\phi = 0.05$ and 0.08, the forward bifurcation in Fig. 2(a) emerges. Figure 2(b) is obtained by the numerical solutions of system (5) at $t = 3000$ under various initial values [$E(0) = 0.05$, $I(0) = 0.02$ or 0.35], which verifies the stability of the equilibrium existing in system (5). The results at $\phi = 0.2$ also indicate the existence of the bistable state (the disease-free equilibrium coexists with an endemic equilibrium). In this situation, given $\beta_1 = 0.18$, i.e., $\beta_1^0 < \beta_1 < \beta_1^c$, there are there equilibria in Fig. 2(a), including a disease-free equilibrium F_0, and two endemic equilibria F_1 and F_2. According to Theorem 3, the equilibria F_0 and F_1 are stable, whereas F_2 is unstable, which results in the bistable state in Fig. 2(b) under $\beta_1 = 0.18$. Figure 3(b) shows the numerical solutions of system (5) under different initial values, in which red, purple,

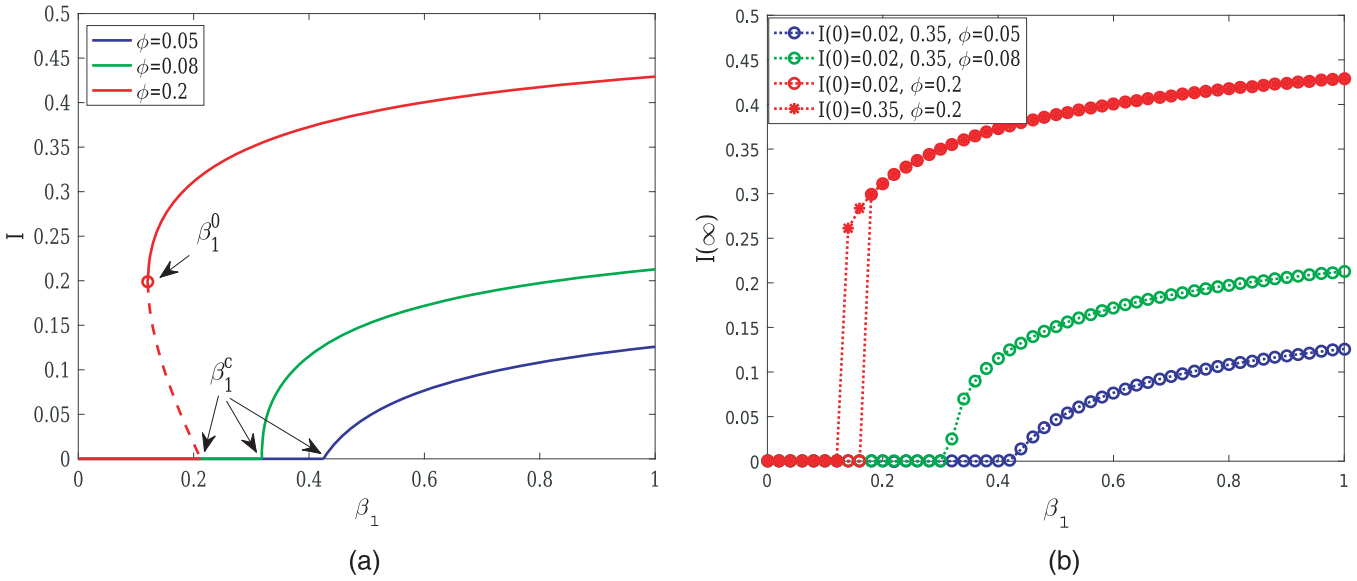

FIG. 2. (a) The equilibria of system (5) under disparate birth rates ϕ. (b) The numerical solutions of system (5) at $t = 3000$ under disparate birth rates ϕ and the initial densities of infected state $I(0)$, where $I(0) = 0.02$ or 0.35, and $E(0) = 0.05$. For both cases, we set $\beta_2 = 0.7$, $\gamma = 0.65$, $\rho = 0.1$, $\alpha = 0.2$, $\langle k_1 \rangle = 6$, and $\langle k_2 \rangle = 10$.

and black points denote the disease-free equilibrium F_0, endemic equilibrium F_1 and F_2, respectively. Obviously, system (5) tends to F_0 or F_1, which is determined by the initial values. Tending to the disease-free equilibrium F_0 in system means that the disease eventually disappears. Reaching the endemic equilibrium F_1 indicates that the disease breaks out and the density of infected nodes remains at a certain value ultimately. When $\beta_1 = 0.1$, i.e., $\beta_1 < \beta_1^0$, system (5) has a disease-free equilibrium F_0 and it is a stable equilibrium, which implies that the system tends to F_0. However, when $\beta_1 = 0.25$, i.e., $\beta_1 > \beta_1^c$, there is endemic equilibrium F_1 in system (5). Finally, system (5) reaches F_1 finally in Fig. 3, since F_1 is stable. On the whole, the forward bifurcation turns into the backward bifurcation as the birth rate ϕ increases, thereby making the emergence of the bistable state. We also find that the outbreak threshold β_1^c decreases with the increase of the birth rate ϕ in Fig. 2(a), and when $\beta_1 > \beta_1^c$ (i.e., after the outbreak of epidemic) and β_1 is fixed, the value of endemic equilibrium increases. Figure 4 exhibits the numerical solutions of system (5) at $t = 3000$ with respect to the pairwise transmission rate

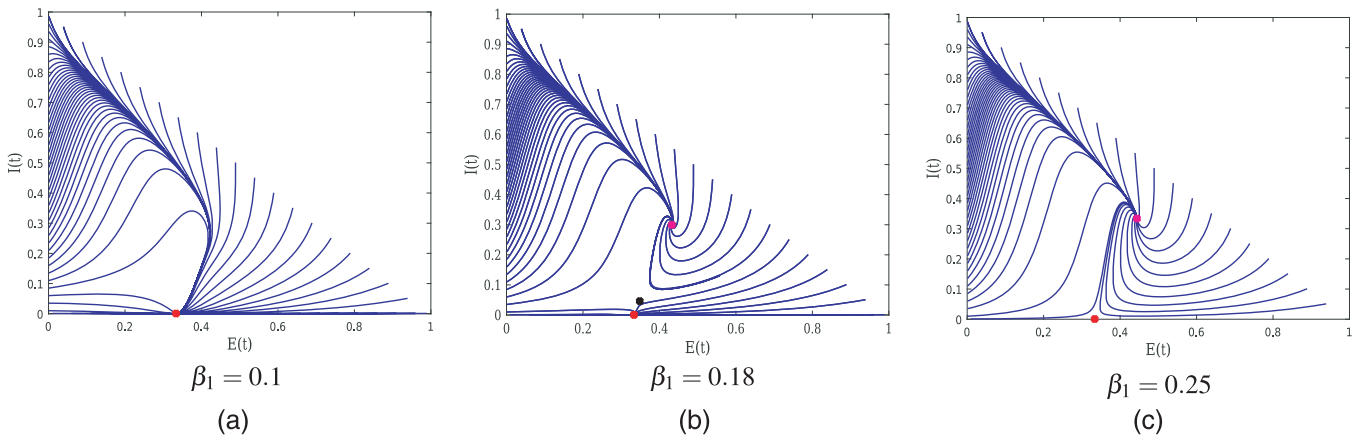

FIG. 3. The numerical solutions of system (5) under different initial values, where $\beta_2 = 0.7$, $\gamma = 0.65$, $\phi = 0.2$, $\rho = 0.1$, $\alpha = 0.2$, $\langle k_1 \rangle = 6$, and $\langle k_2 \rangle = 10$. (a) $\beta_1 = 0.1$, (b) $\beta_1 = 0.18$, (c) $\beta_1 = 0.25$.

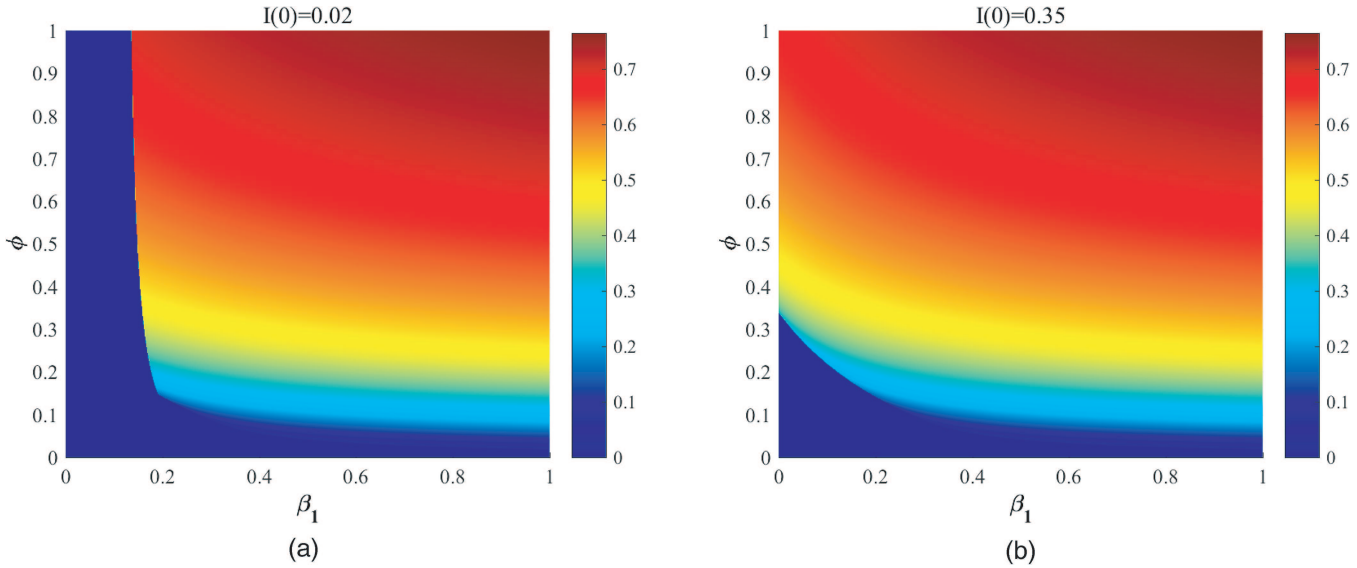

FIG. 4. The numerical solutions of system (5) at $t = 3000$ with respect to the pairwise transmission rate β_1 and birth rates ϕ, where $I(0) = 0.02$ and 0.35 in (a) and (b), respectively, and the values of other parameters are the same as in Fig. 2.

β_1 and birth rates ϕ, which provides validation for the results about the influences of birth rates.

Furthermore, to identify the dynamics of system (5) under the specific birth rate ϕ and the pairwise transmission rate β_1, we analyze the relations between the birth rate and the thresholds β_1^0 and β_1^c based on Eqs. (6) and (7), respectively. In Fig. 5, the red and blue curves denote the values of β_1^0 and β_1^c under different birth rates, respectively, which divides the whole area into three regions, labeled by (1), (2) and (3), respectively. In region (1), $\beta_1 < \beta_1^0$ and $\beta_1 < \beta_1^c$, which implies that system (5) only has a stable disease-free equilibrium in Fig. 2(a), thereby tending to the disease-free state. In region (2), $\beta_1^0 < \beta_1 < \beta_1^c$, and the stable disease-free and endemic equilibria coexist, which indicates that the bistable state appears. Reaching to the disease-free state or the endemic state depends on the initial values of system (5), as shown in Fig. 3(b). In region (3), $\beta_1 > \beta_1^c$, and there are only the stable endemic equilibria in system (5), thereby reaching the endemic state. The regions in Fig. 5 are in agreement with Fig. 4. Hence, when ϕ and β_1 are fixed, we can determine the dynamical region which the parameters belong to, thereby obtaining the dynamics of system (5). On the whole, when β_1 through β_1^0, the number of endemic equilibrium in system (5) goes from 0 to 2. Therefore, a saddle-node bifurcation appears in system (5) when $\beta_1 = \beta_1^0$. If β_1 goes through β_1^c, the stable state of system (5) changes from the disease-free state to the endemic state, which indicates that a transcritical bifurcation is present in system (5) when $\beta_1 = \beta_1^c$.

Similarly, we demonstrate the appearance of the backward bifurcation with the increase of the death rates ρ and α in Figs. 6(a) and 7(a), as well as the occurrence of the bistable state in Figs. 6(b) and 7(b), respectively. According to Eq. (6), the outbreak threshold β_1^c increases as ρ and α increase, which is also demonstrated in Figs. 6(a) and 7(a). Meanwhile, the value of endemic equilibrium decreases when $\beta_1 > \beta_1^c$ and β_1 is fixed.

We, therefore, conclude that the values of birth and death rates can influence the existence and stability of the disease-free equilibrium and the endemic equilibrium, thereby determining the backward and forward bifurcations, which is the crucial reason of the existence or absence of the bistable state. Moreover, the outbreak

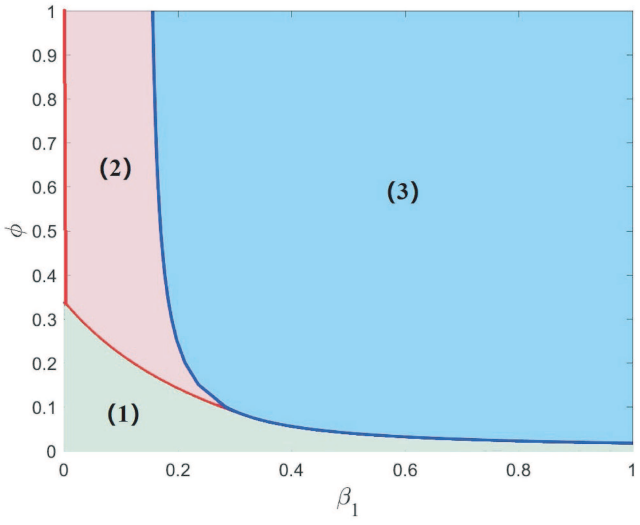

FIG. 5. The regions are divided by thresholds β_1^0 and β_1^c. The values of parameters are the same as in Fig. 4.

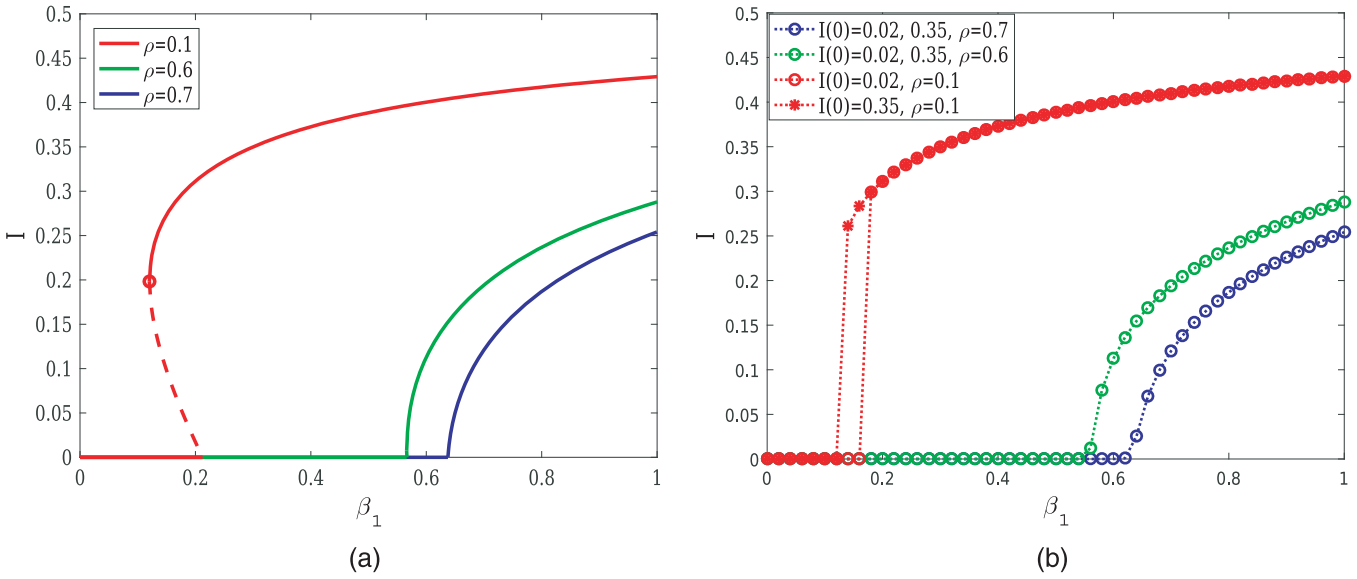

FIG. 6. (a) The equilibria of system (5) under disparate death rates ρ. (b) The numerical solutions of system (5) at $t = 3000$ under disparate death rates ρ and the initial densities of infected state $I(0)$, where $I(0) = 0.02$ or 0.35, and $E(0) = 0.05$. For both cases, we set $\beta_2 = 0.7$, $\gamma = 0.65$, $\phi = 0.2$, $\alpha = 0.2$, $\langle k_1 \rangle = 6$, and $\langle k_2 \rangle = 10$.

threshold and the infected stationary state also vary with the birth and death rates.

The above simulations show that the endemic equilibrium F_1 is locally stable, thereby tending to the endemic state for the disease. In theoretical analysis, the endemic equilibrium F_1 is locally stable only under certain conditions, which implies that F_1 is not always stable. In order to further explore the dynamics of the system (5) when F_1 is unstable, more numerical simulations are conducted, as shown in Fig. 8, where a stable periodic solution of system (5) emerges at some initial conditions. Under this scenario, system (5) presents a bistable state, coexisting a stable periodic solution and a steady disease-free equilibrium.

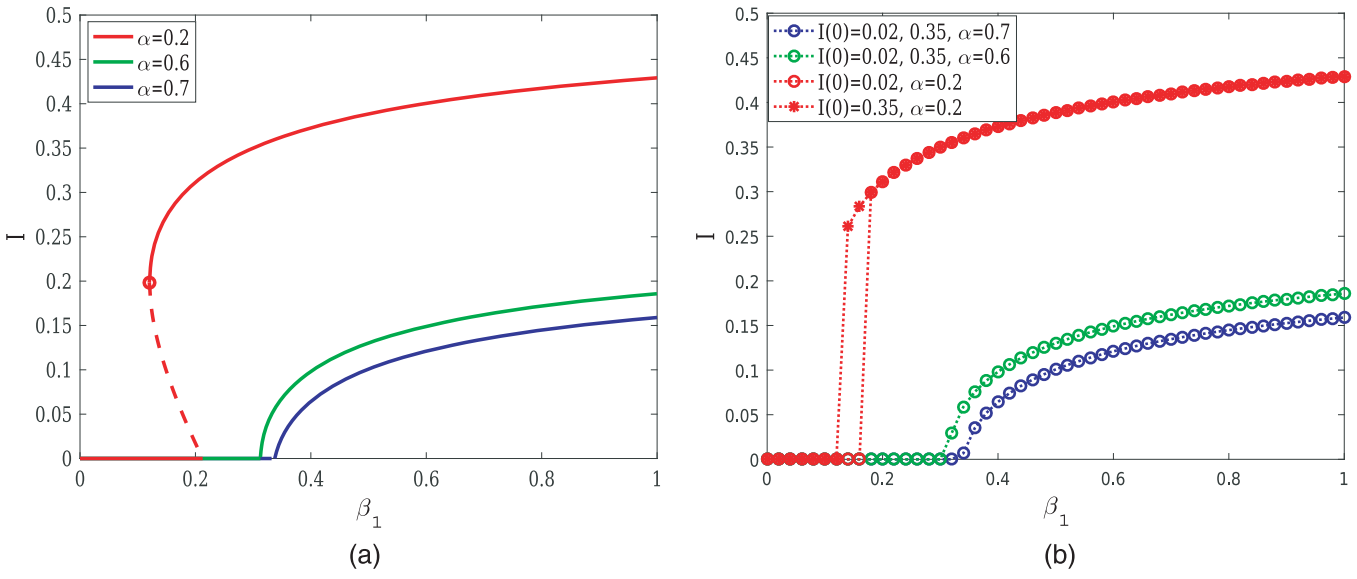

FIG. 7. (a) The equilibria of system (5) under disparate death rates due to the disease α. (b) The numerical solutions of system (5) at $t = 3000$ under disparate death rates due to the disease α and the initial densities of infected state $I(0)$, where $I(0) = 0.02$ or 0.35, and $E(0) = 0.05$. For both cases, we set $\beta_2 = 0.7$, $\gamma = 0.65$, $\phi = 0.2$, $\rho = 0.1$, $\langle k_1 \rangle = 6$, and $\langle k_2 \rangle = 10$.

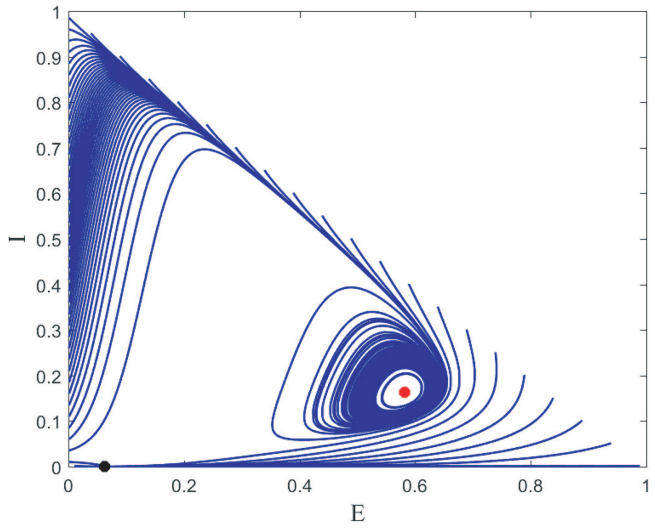

FIG. 8. The coexistence of a stable periodic solution and a steady disease-free equilibrium of system (5), where $\beta_1 = 0.1$, $\beta_2 = 0.98$, $\gamma = 0.39$, $\phi = 0.15$, $\rho = 0.01$, $\alpha = 0.52$ $\langle k_1 \rangle = 6.5974$, and $\langle k_2 \rangle = 18.1948$.

IV. NUMERICAL SIMULATIONS ON EMPIRICAL NETWORKS

In the above section, the dynamics of system (4) is analyzed by the MF method under a homogeneous mixing hypothesis of system (2). Since system (2) is the quenched mean-field model combining with network topology, it can characterize epidemic spreading on empirical networks. Under the guidance of the theoretical analysis of system (4), we specifically discuss the spreading process on different empirical networks in this section. Extensive numerical simulations illustrate that the theoretical results obtained by the MF method provide guidance implication for the heterogeneous models. The synthetic scale-free network[21] and coauthorship network of scientists working on network theory and experiment[22] are chosen. In simulations, we only consider the dimension of the simplex in networks up to 2. In a network, the edge between the two nodes is deemed to be a 1-simplex. If there are edges between any two of three nodes, the three nodes and their connections forms a triangle, which is regarded as a 2-simplex. The statistical characteristics of the two networks are shown in Table I. Parameters N, $\langle k_1 \rangle$, and $\langle k_2 \rangle$ denote the number of sites, the average degree, and the average number of 2-simplices, respectively.

TABLE I. Statistical properties of networks.

Network	N	$\langle k_1 \rangle$	$\langle k_2 \rangle$
Scale-free network	1000	6	0.864
Coauthorship network	1589	3.4512	6.9893

Initially, we randomly choose a fraction of sites $I(0)$ occupied by infected individuals and a fraction of sites $E(0)$ is empty, while others are occupied by susceptible individuals. Here, we set $E(0) = 0.1$. For simplicity, we only consider the dimension of simplices up to 2. Once all states reach steady states, the simulation

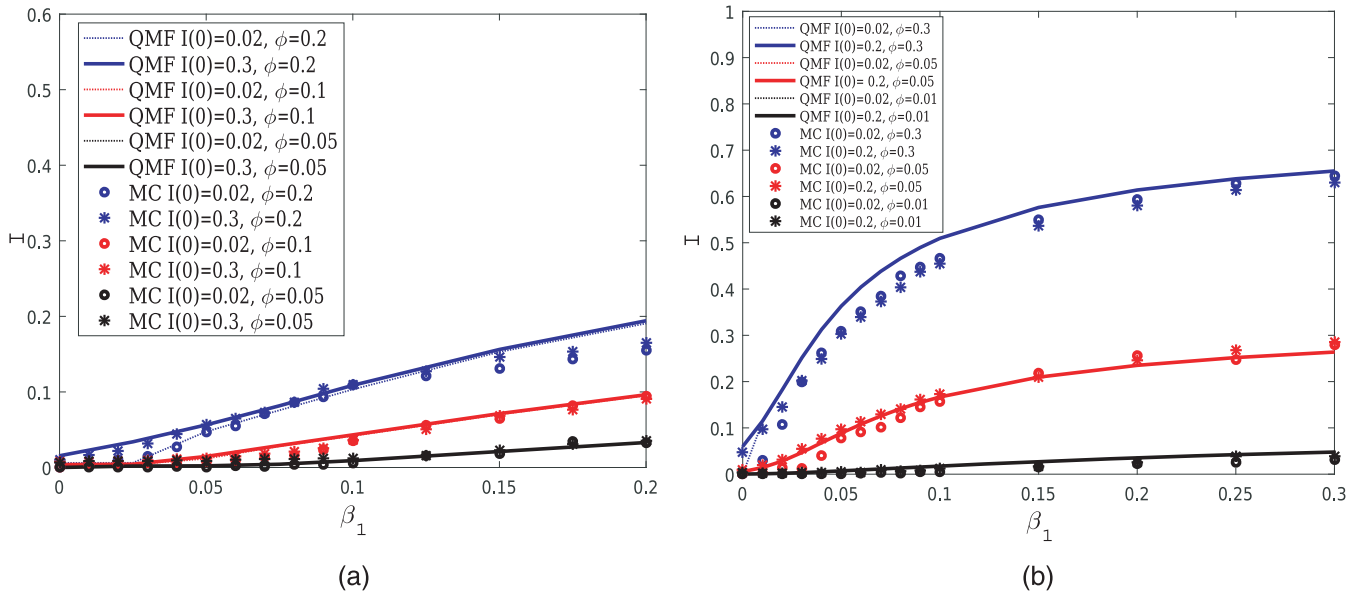

FIG. 9. The density of infected nodes in the stationary state vs the pairwise transmission rate β_1 under disparate birth rates ϕ and initial densities of the infected state $I(0)$. Here, we set $\beta_2 = 0.1$, $\gamma = 0.05$, $\rho = 0.1$, $\alpha = 0.2$ in coauthorship networks [Fig. 9(a)], and $\beta_2 = 0.2$, $\gamma = 0.05$, $\rho = 0.05$, $\alpha = 0.1$ in scale-free networks [Fig. 9(b)]. The red and black dotted lines overlap with the solid lines of the corresponding colors. (a) Coauthorship network, (b) scale-free network.

process terminates. At each time t, the density of infected individuals is $I(t) = \frac{1}{N}\sum_{i=1}^{N} I_i(t)$.

Figure 9 shows the density of infected nodes in the stationary state vs the transmission rate through 1-simplex β_1 over the above two networks, under disparate birth rates ϕ and initial densities of the infected state $I(0)$. The curves and symbols represent the results of the quenched mean-field method (QMF method) and the Monte Carlo method (MC method). For sake of showing the bistable state, we only take a part of values β_1.

In Fig. 9(a), when $\phi = 0.2$, there are deviations on the simulated curves for the initial values $I(0) = 0.02$ and 0.3. Under $\beta_1 = 0$, it is observed that $I(\infty) > 0$ when $I(0) = 0.3$, while $I(\infty) = 0$ when

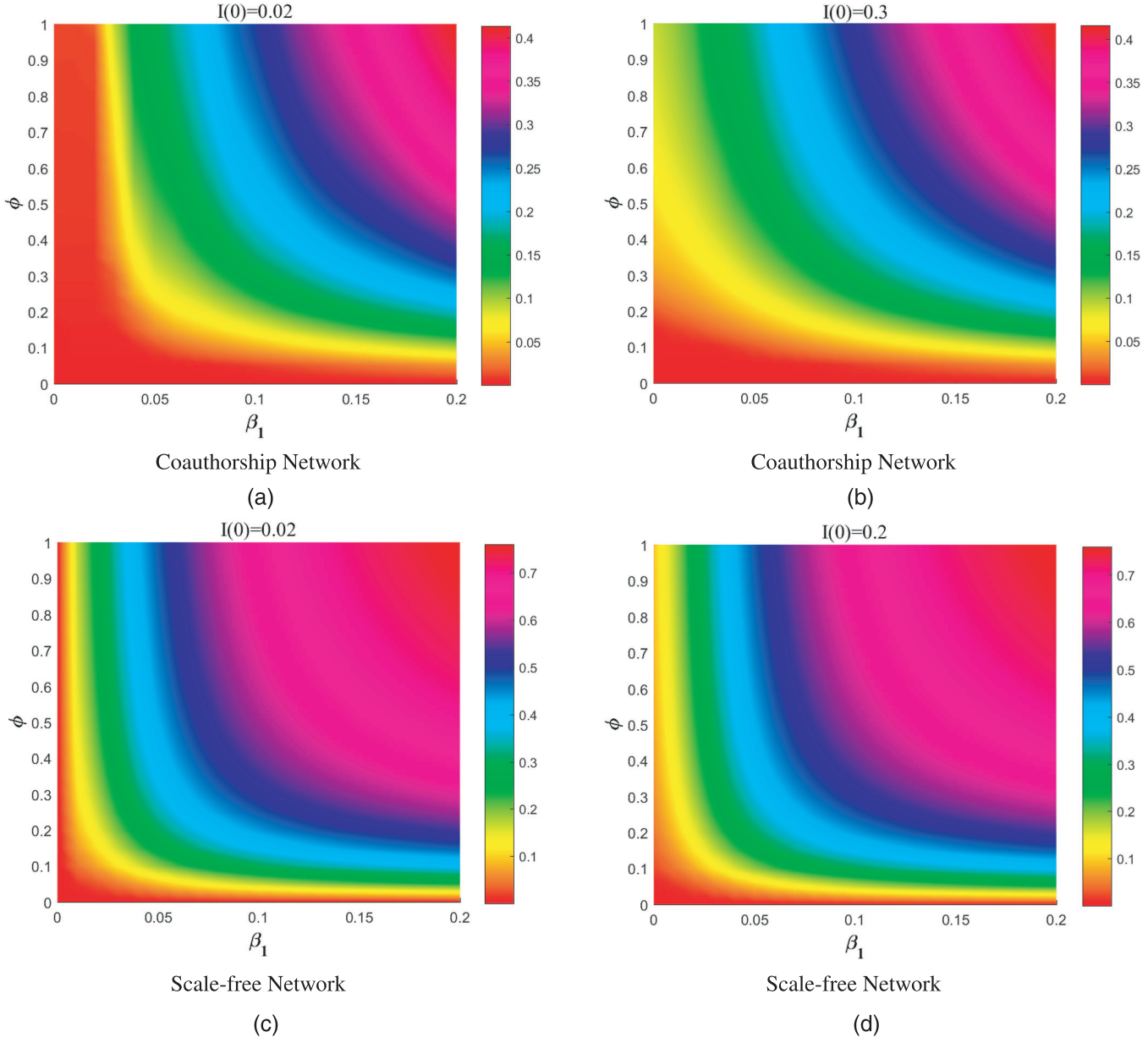

FIG. 10. The density of infected nodes in the stationary state with respect to the pairwise transmission rate β_1 and birth rates ϕ under disparate initial densities of infected state $I(0)$, where parameter values are the same as in Fig. 9. Figures 10(a) and 10(b) are the results of the quenched mean-field method in coauthorship networks, where the initial value is $I(0) = 0.02$ and 0.3, respectively. Figures 10(c) and 10(d) are the results of the quenched mean-field method in scale-free networks, where the initial value is $I(0) = 0.02$ and 0.2, respectively. (a) Coauthorship network, (b) coauthorship network, (c) scale-free Network, (d) scale-free network.

$I(0) = 0.02$. The disease breaks out earlier when $I(0) = 0.3$ than when $I(0) = 0.02$, and the disease-free state $I(\infty) = 0$ and endemic state $I(\infty) > 0$ coexist when $0 < \beta_1 < 0.025$, thereby indicating the bistable state. However, when $\phi = 0.05$ and 0.1, the simulated curves are coincident whatever the value of $I(0)$ is. However, on the whole, the bistable state fades away on decreasing ϕ by comparing Figs. 10(a) and 10(b). Such a phenomenon is associated with the bifurcation diagram in Fig. 2(a), which presents the change from the backward bifurcation to forward bifurcation as ϕ decreases, just corresponding to the disappearance of the bistable state. The similar phenomenon also occurs in scale-free networks [Figs. 9(b), 10(c), and 10(d)]. Figure 10(b) shows that the smaller the birth rate ϕ is, the bigger the outbreak threshold is, and the density of infected nodes in the stationary state decreases with the decrease of the birth rate ϕ when β_1 is fixed, which is consistent with results in Fig. 4(b).

Then, we explore the effect of death rates on epidemic spreading. Obviously, the bistable state exists when $\rho = 0.1$, 0.3 in Fig. 11(a) and when $\alpha = 0.2$ in Fig. 13(a), while it disappears when $\rho = 0.5$ and $\alpha = 0.3$, 0.4. A similar phenomenon takes place in Figs. 11(b) and 13(b), which show that the bistable state vanishes as ρ or α increases. Further, when β_1 and ρ (α) change simultaneously, the density of infected nodes in the stationary state is shown in Fig. 12 (Fig. 14), which confirms that the increase of death rates results in an increase of the outbreak threshold, and the density of infected nodes in the stationary state decreases when β_1 is fixed.

In conclusion, the change of birth and death rates affects the existence of bistable state on empirical networks, where the decrease of birth rates or the increase of death rates makes the bistable state disappear. Furthermore, birth and death rates can shift the outbreak threshold and the density of infected nodes in the stationary state. Specifically, the outbreak threshold increases and the value of the infected stationary state decreases with the decrease of birth rates or increase of death rates, thereby effectively suppressing epidemic spreading. The above conclusions about the effect of the birth and death on simplicial SIS epidemic spreading are consistent with the theoretical analysis of the mean-field system (5). It indicates that the theoretical conclusions of the system (5) are applicable to the quenched mean-field system (2), thereby providing the guidance for the network-based models (2).

It is observed that the results of the QMF method agree with the MC method on the whole in Figs. 9, 11, and 13, which indicates the QMF method is an effective approximation method. Note that the slight deviations of results between the QMF method and MC method are due to the assumption of the QMF method that the probability of being infected by one neighbor is independent of the probability of being infected by any other neighbor. Once the two neighbors (neighbors j and k) of node i connect, there exists a 2-simplex ($[i, j, k]$) on node i. When node i is infected through the high-order interaction of the 2-simplex, we assume that neighbors j and k are all in the infected state, which is denoted by the product of infected probabilities of neighbors j and k in the quenched mean-field equation (2). In fact, there are interactions between neighbors j and k, which indicates that the product of infected probabilities of neighbors j and k is an approximate value of the infected probability of neighbors j and k at the same time. Hence, it seems that the existence of more high-order structures makes the assumption less satisfied. In simulations, the average number of 2-simplices in the coauthorship network is obviously greater than scale-free network,

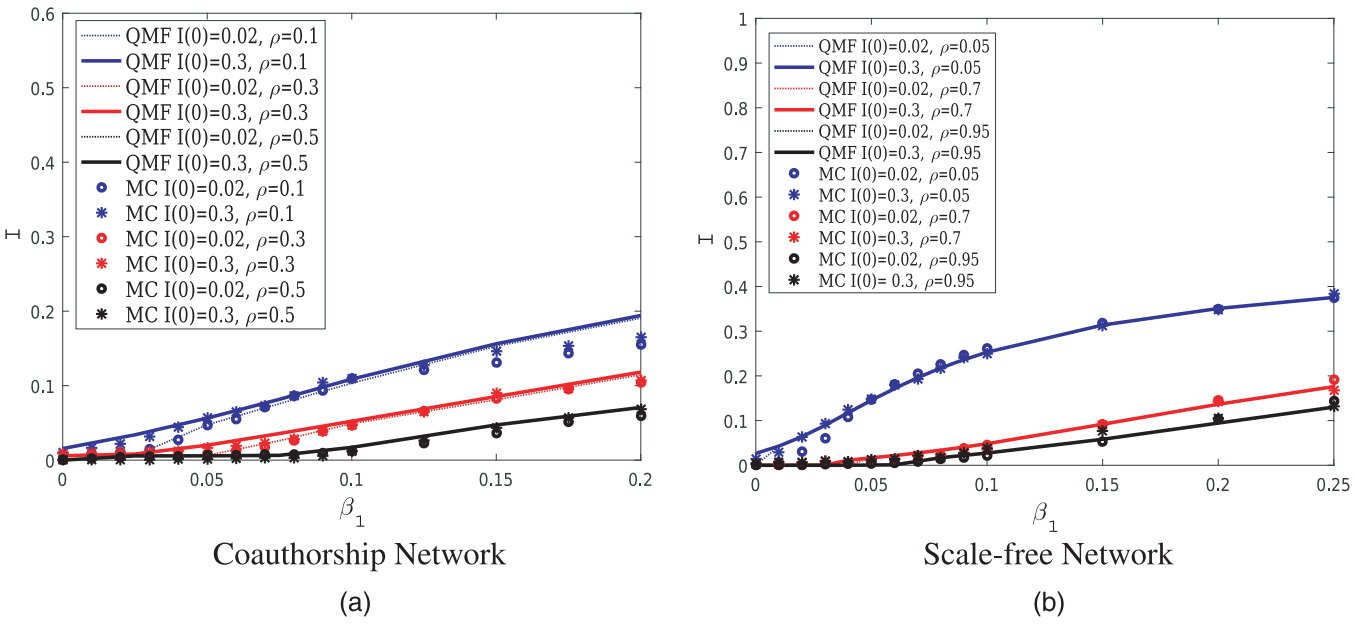

FIG. 11. The density of infected nodes in the stationary state vs the pairwise transmission rate β_1 under disparate death rates ρ and initial densities of the infected state $I(0)$. Here, we set $\beta_2 = 0.1$, $\gamma = 0.05$, $\phi = 0.2$, $\alpha = 0.2$ in coauthorship networks [Fig. 11(a)], and $\beta_2 = 0.35$, $\gamma = 0.05$, $\phi = 0.2$, $\alpha = 0.2$ in scale-free networks [Fig. 11(b)]. (a) Coauthorship network, (b) scale-free network.

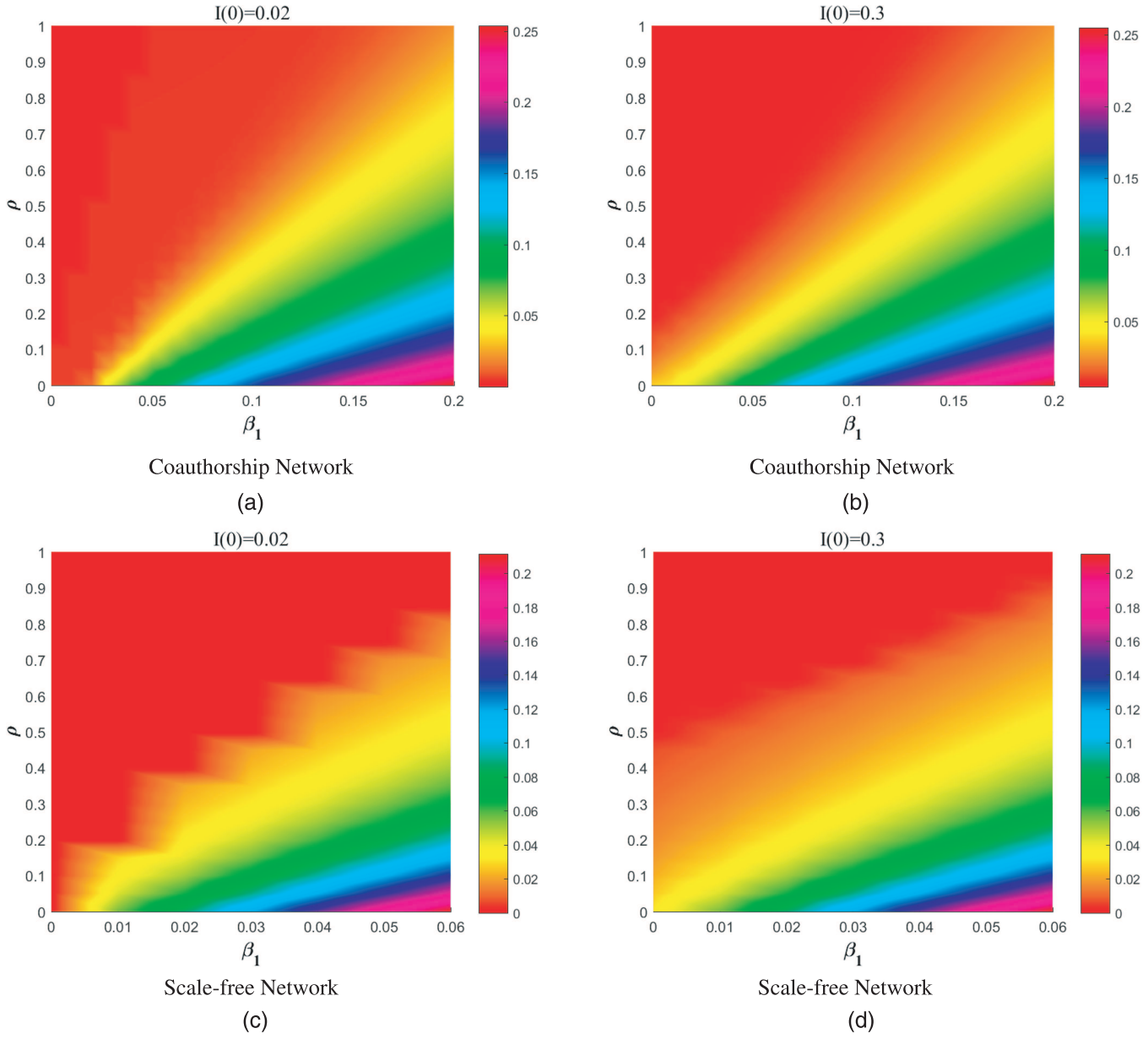

FIG. 12. The density of infected nodes in the stationary state with respect to the pairwise transmission rate β_1 and death rates ρ under disparate initial densities of infected state $I(0)$, where parameter values are the same as in Fig. 11. Figures 12(a) and 12(b) are the results of the quenched mean-field method in coauthorship networks, where the initial value is $I(0) = 0.02$ and 0.3, respectively. Figures 12(c) and 12(d) are the results of the quenched mean-field method in scale-free networks, where the initial value is $I(0) = 0.02$ and 0.3, respectively. (a) Coauthorship network, (b) Coauthorship network, (c) scale-free network, (d) scale-free network.

which causes that the dynamical correlation between neighbors in the coauthorship network have a greater influence than the scale-free networks. Hence, when β_1 is big enough, the deviations of results about the QMF method and MC method become large in the coauthorship network, while there are no deviations in the scale-free network.

In this paper, we focus on theoretical analysis of the dynamical phenomena about the effect of the birth and death. The quenched mean-field equation well maintains the theoretical properties and conclusion of epidemic spreading when it is reduced as the mean-field system to. The analysis based on the mean-field system can well explain the dynamic behaviors in networks theoretically. Therefore,

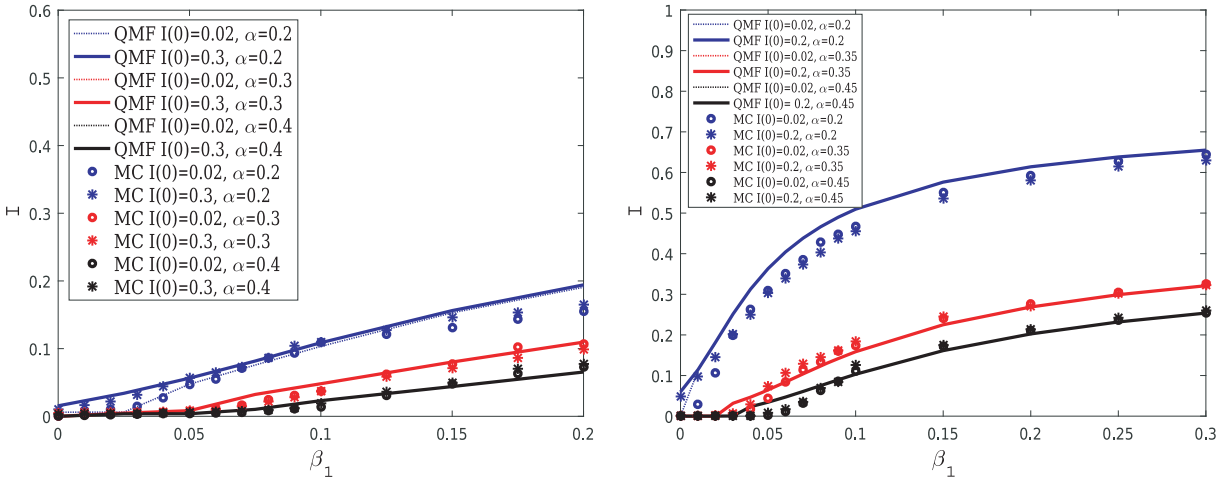

FIG. 13. The density of infected nodes in the stationary state vs the pairwise transmission rate β_1 under disparate death rates α and the initial densities of infected state $I(0)$. Here, we set $\beta_2 = 0.1$, $\gamma = 0.05$, $\phi = 0.2$, $\rho = 0.1$ in Coauthorship Network [Fig. 13(a)], and $\beta_2 = 0.2$, $\gamma = 0.05$, $\phi = 0.3$, $\rho = 0.05$ in Scale-free Network [Fig. 13(b)]. (a) Coauthorship Network, (b) Scale-free Network.

we adopt the quenched mean-field method to address epidemic spreading based on pairwise and high-order interactions in this paper. In the future studies, we will address the limitation of the quenched mean-field equation (2) by epidemic link equations, which are studied to model social contagion or epidemic spreading, which make the models more accurate to describe the propagation process.[15]

In the above dynamical phenomena, the spread of the disease ends up in the disease-free state or endemic state, which depends on initial conditions of system (2) and the values of parameters including the birth and death rates ϕ, ρ, α and 2-simplex spreading rate β_2. Nevertheless, the endemic state is not always stable, which implies periodic phenomenon of epidemic outbreaks may emerge. As an instance, in Fig. 15, we present the stable periodic outbreak and disease-free states in Les Miserables Network,[23] which verifies that the same phenomenon in Fig. 8 occurs on the specific network. In this case, system (2) eventually reaches a periodic oscillation or a infection-free stationary state, which depends on initial conditions.

Finally, we observe the effect of network topology on the epidemic threshold. In Fig. 16, the red, blue and black dots are the epidemic thresholds in scale-free networks with the average degree $\langle k_1 \rangle = 4$, 6, and 10, respectively. It is observed that the epidemic threshold increases as the average degree decreases, which implies they are negatively correlated. The simulated results demonstrate that the network topology has an effect on the epidemic spreading.

V. SENSITIVITY ANALYSIS

A. Outbreak threshold

Increasing the outbreak threshold is a way to prevent disease outbreak. Intuitively, the outbreak threshold β_1^c is related to a number of parameters in Eq. (6), including ϕ, ρ, α, γ and $\langle k_1 \rangle$, which means that figuring out how the parameters affect β_1^c is pivotal to control. The impact of parameters on β_1^c can be described by the elasticity of quantity about parameters, which is defined as follows:

Definition 1. [24]The elasticity of quantity of Q with respect to the parameter q is given by

$$\varepsilon_Q^q = \frac{\partial Q}{\partial q}\frac{q}{Q}. \tag{8}$$

On the basis of the definition, we derive the elasticity of β_1^c with respect to a given parameter. Further, we numerically compute the related results, which are presented in Table II. It shows that ϕ and $\langle k_1 \rangle$ are negatively correlated with β_1^c, which implies β_1^c increases as ϕ or $\langle k_1 \rangle$ decrease. On the contrary, ρ, α, and γ are positively correlated, and the increase of them leads to the increase of β_1^c. The correlation analysis between the parameters and β_1^c well verifies the impact of birth and death on outbreak threshold in Sec. IV. Appropriate reductions of ϕ, $\langle k_1 \rangle$ or increases of ρ, α,γ can increase the outbreak threshold, thereby preventing disease outbreak. Furthermore, the largest and least impacts on the threshold are $\langle k_1 \rangle$ and α, respectively, where an increase of 10% in $\langle k_1 \rangle$ can result in a decrease of β_1^c by 10%, while an increase of 10% in α leads to a increase of β_1^c by 2.173 913%. Thus, reducing $\langle k_1 \rangle$ is a better way for inhibiting disease outbreaks than changing other parameters.

B. Dynamic behaviors

It is clear that how the related parameters affect the outbreak threshold. Furthermore, since parameters also influence the

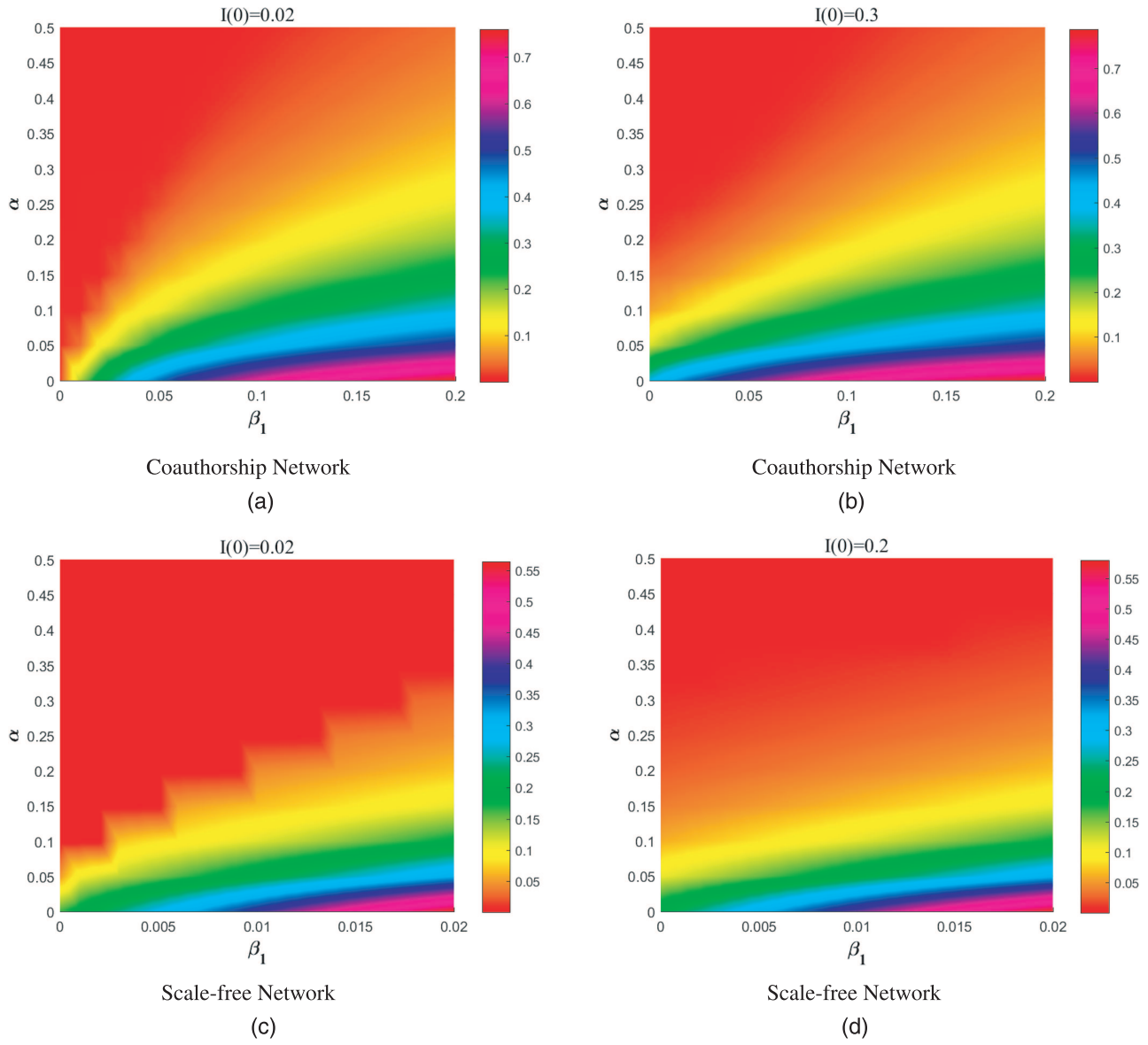

FIG. 14. The density of infected nodes in the stationary state with respect to the pairwise transmission rate β_1 and death rates α under disparate initial densities of infected state $I(0)$, where parameter values are the same as in Fig. 13. Figures 14(a) and 14(b) are the results of the quenched mean-field method in Coauthorship Network, where the initial value is $I(0) = 0.02$ and 0.3, respectively. Figures 14(c) and 14(d) are the results of the quenched mean-field method in Scale-free Network, where the initial value is $I(0) = 0.02$ and 0.2, respectively. (a) Coauthorship Network, (b) Coauthorship Network, (c) Scale-free Network, (d) Scale-free Network.

dynamic behaviors of system, the sensitivity analysis of system in regard to all parameters is necessary, which is conducted based on the sensitivity analysis system.

The partial derivative of $X = (E, I)^T$ with regard to a parameter $p \in \{\phi, \rho, \alpha, \gamma, \beta_1, \beta_2, \langle k_1 \rangle, \langle k_2 \rangle\}$ is defined as the sensitivity analysis system of model (5) about p, denoted by $X_p = \frac{\partial X}{\partial p}$. We thus obtain the following sensitivity analysis system:

$$\begin{aligned} \frac{dX}{dt} &= h(X), \\ \frac{dX_p}{dt} &= \frac{dh}{dX} X_p + \frac{\partial h}{\partial p}. \end{aligned} \tag{9}$$

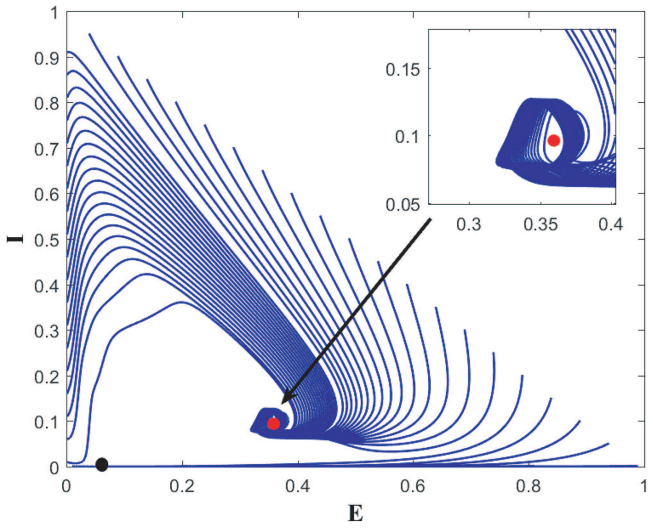

FIG. 15. The periodic outbreak of epidemic and the stable disease-free state coexist in Les Miserables Network, where $\beta_1 = 0.1$, $\beta_2 = 0.98$, $\gamma = 0.95$, $\phi = 0.15$, $\rho = 0.01$, and $\alpha = 0.52$.

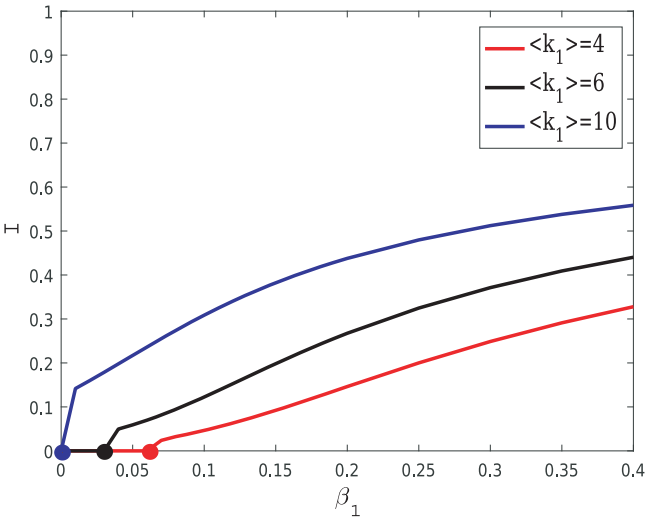

FIG. 16. The effect of the average degree on the epidemic threshold $\beta_1^{c(net)}$ in scale-free networks, where $I(0) = 0.02$, $E(0) = 0.1$, $\beta_2 = 0.4$, $\gamma = 0.7$, $\phi = 0.3$, $\rho = 0.05$ and $\alpha = 0.1$.

According to Ref. 25, the semi-relative sensitivity solutions describe the change of the state variables if the parameter is doubled, which is calculated by pX_p. And the logarithmic sensitivity solutions $\frac{pX_p}{X}$ represent the variation percentage that can be expected from a doubling of the parameter.

Figures 17(a) and 17(b) show the semi-relative sensitivity solutions of E and I, respectively. The curve about β_2 coincides with $\langle k_2 \rangle$ in Fig. 17 (Fig. 18). In Fig. 17(a), it is obvious that $\rho, \beta_2, \langle k_1 \rangle$, and $\langle k_2 \rangle$ have a positive effect on the variable E, while ϕ and γ have an

TABLE II. Parameter values of system and elasticity of β_1^c.

Parameter	Value	Elasticity
ϕ	0.2	−0.428 571 4
ρ	0.15	0.428 571 4
α	0.25	0.217 391 3
γ	0.9	0.782 608 7
$\langle k_1 \rangle$	6.5974	−1

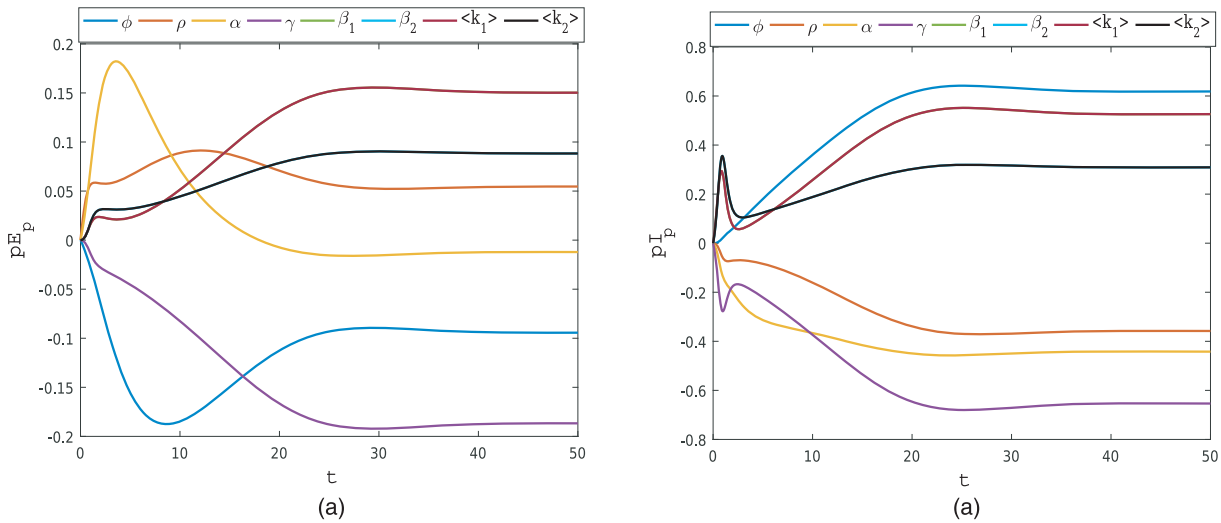

FIG. 17. The semi-relative sensitivity solutions of E (a) and I (b) with respect to the parameter $p \in \{\phi, \rho, \alpha, \gamma, \beta_1, \beta_2, \langle k_1 \rangle, \langle k_2 \rangle\}$.

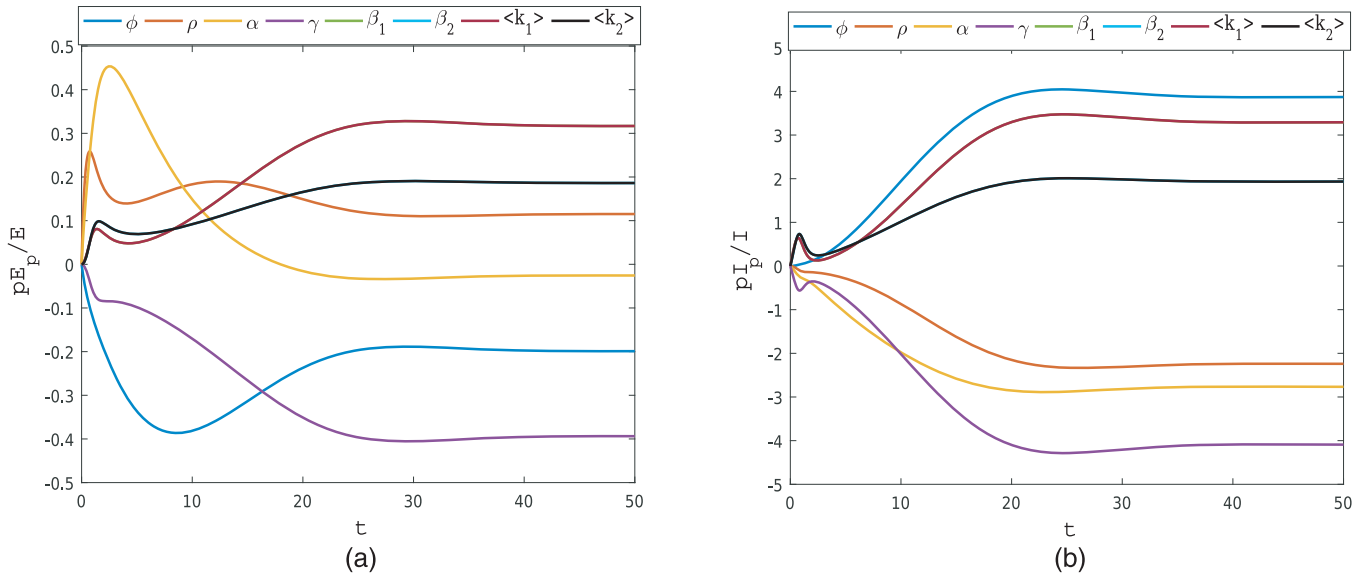

FIG. 18. The logarithmic sensitivity solutions of E (a) and I (b) with respect to the parameter $p \in \{\phi, \rho, \alpha, \gamma, \beta_1, \beta_2, \langle k_1 \rangle, \langle k_2 \rangle\}$.

opposite effect. We observe that the curve of α crosses the zero-line at certain t, which means that the doubling of α will cause that E increases in the initial stage, and then decreases. α has the largest positive effect on E at $t = 4$, while ϕ has the largest negative effect at $t = 8$. The effect of parameters tends to stabilize at a certain value after $t = 25$. In Fig. 17(b), the perturbations of $\phi, \beta_2, \langle k_1 \rangle$, and $\langle k_2 \rangle$ will cause an increase of I, while the effect of ρ, α, and γ are opposite, which further verifies the previous finding that the density of the infected stationary state decreases with the decrease of birth rates or increase of death rates in Sec. IV. The effect of parameters excepting β_2 and $\langle k_2 \rangle$ on I is maximum at $t = 25$ and subsequently tends to stabilize. The maximum influence of β_2 and $\langle k_2 \rangle$ occurs at $t = 2$.

From the logarithmic sensitivity solutions of E and I in Fig. 18, we observe that the effect ways (positive or negative effects) of parameters is analogous with the the semi-relative sensitivity solutions in Fig. 17, respectively. What is different from Fig. 17 is the impacts of β_2 and $\langle k_2 \rangle$ on E and I reach the maximum value at $t = 25$, and they tend to stabilize subsequently.

To sum up, there is no doubt that the birth and death of individuals are vital for dynamical behaviors. The positive effect of birth rate ϕ on the density of infected signifies that decreasing ϕ inhibits the disease spread, while the negative effect of the death rates ρ and α illustrates that increasing them can suppress the epidemic spread.

VI. CONCLUSION

In this paper, a simplicial epidemic model with consideration of birth and death is investigated, in which epidemic spreads not only through edge, but also high-order structures. Since birth and death can change the total number of individuals, we introduce empty sites to keep the total number of sites invariant, thereby developing a simplicial SIS epidemic model with birth and death. Based on the proposed model, we get the probabilistic evolution equations of each site being in the empty, susceptible, and infected states, respectively, by the quenched mean-field method. Remarkably, theoretical analysis of equilibrium shows the decrease of birth rates or the increase of death rates makes the bistable state disappear, which are also demonstrated by extensive simulations on empirical and synthetic networks. Meanwhile, the outbreak threshold increases and the density of infected nodes in the stationary state decrease as birth rates decrease or death rates increase, thereby suppressing the epidemic spread, which is verified by sensitivity analysis of the proposed model. In addition, the steady periodic outbreak emerges coexisting with a stable disease-free state when the birth, death rates, and other parameters satisfy the certain conditions, thereby springing up another type of the bistable state.

ACKNOWLEDGMENTS

This work was supported by the Natural Science Foundation of Guangdong, China under Grant Nos. 2020A1515010812 and 2021A1515011594.

AUTHOR DECLARATIONS

Conflict of Interest

The authors have no conflicts to disclose.

Author Contributions

Hui Leng: Conceptualization (equal); Data curation (equal); Methodology (equal); Software (equal); Writing – original draft (equal); Writing – review & editing (equal). **Yi Zhao:** Conceptualization (equal); Funding acquisition (equal); Supervision (equal);

Writing – review & editing (equal). **Jianfeng Luo:** Conceptualization (equal); Supervision (equal); Writing – review & editing (equal). **Yong Ye:** Software (equal); Writing – review & editing (equal).

DATA AVAILABILITY

The data that support the findings of this study are available from the corresponding author upon reasonable request.

APPENDIX: DYNAMICWS ANALYSIS

Here, we discuss the existence and stability of equilibria of system (5).

1. Existence of equilibria

Let $\frac{dE}{dt} = 0$ and $\frac{dI}{dt} = 0$ in system (5). Then, we get its equilibria based on the following equations:

$$\begin{aligned} &-(\phi+\rho)E(t) + (\alpha-\rho)I(t) + \rho = 0, \\ &\beta_1\langle k_1\rangle - \gamma - \alpha - \beta_1\langle k_1\rangle E(t) - \beta_2\langle k_2\rangle E(t)I(t) + (\beta_2\langle k_2\rangle \\ &\quad - \beta_1\langle k_1\rangle)I(t) - \beta_2\langle k_2\rangle I^2(t) = 0. \end{aligned} \tag{A1}$$

First, let $I = 0$ in Eq. (A1), and then we get a unique disease-free equilibrium $F_0 = \left(\frac{\rho}{\phi+\rho}, 0\right)$, which implies that the spreading dies out.

Then, when $I \neq 0$ in Eq. (A1), we get the endemic equilibria of system (5). Equation (A1) yields

$$E = \frac{\alpha I + (1-I)\rho}{\phi+\rho}. \tag{A2}$$

Since E and I denote the density of empty sites and infected individuals, respectively, only $0 < E < 1$ and $0 < I < 1$ satisfy the biomathematics background of system (5). To ensure the existence and rationality of Eq. (A2), $0 < E < 1$ is required. In terms of Eq. (A2), we get that $E > 0$ is always satisfied since $I < 1$. When $\alpha > \rho$, $E < 1$ is satisfied only if $0 < I < \min\{\frac{\phi}{\alpha-\rho}, 1\}$. When $\alpha < \rho$, $E < 1$ is satisfied only if $0 < I < 1$. Let

$$f(I) = a_1 I^2 + b_1 I + c_1, \tag{A3}$$

where

$$\begin{aligned} a_1 &= -(\phi+\alpha)\beta_2\langle k_2\rangle, \\ b_1 &= \phi\beta_2\langle k_2\rangle - (\phi+\alpha)\beta_1\langle k_1\rangle = (\phi+\alpha)\beta_1\langle k_1\rangle(R_1-1), \\ c_1 &= \phi\beta_1\langle k_1\rangle - (\gamma+\alpha)(\phi+\rho) = -\phi\beta_1\langle k_1\rangle(1-R_0)/R_0, \\ R_0 &= \frac{\phi\beta_1\langle k_1\rangle}{(\gamma+\alpha)(\phi+\rho)}, \quad R_1 = \frac{\phi\beta_2\langle k_2\rangle}{(\phi+\alpha)\beta_1\langle k_1\rangle}. \end{aligned} \tag{A4}$$

The solutions of the second formula in Eq. (A1) are equivalent to the roots of $f(I) = 0$. The discriminant of the roots for $f(I) = 0$ is

$$\begin{aligned} \Delta_1 = b_1^2 - 4a_1c_1 &= ((\phi+\alpha)\beta_1\langle k_1\rangle(R_1-1))^2 \\ &\quad - 4\phi(\alpha+\phi)\beta_1\beta_2\langle k_1\rangle\langle k_2\rangle(1-R_0)/R_0. \end{aligned} \tag{A5}$$

When $\Delta_1 > 0, f(I) = 0$ admits two different roots

$$\begin{aligned} I_1 &= \frac{(\phi+\alpha)\beta_1\langle k_1\rangle(R_1-1) + \sqrt{\Delta_1}}{2(\phi+\alpha)\beta_2\langle k_2\rangle}, \\ I_2 &= \frac{(\phi+\alpha)\beta_1\langle k_1\rangle(R_1-1) - \sqrt{\Delta_1}}{2(\phi+\alpha)\beta_2\langle k_2\rangle}. \end{aligned} \tag{A6}$$

Then, we discuss the existence conditions of the endemic equilibria, i.e., the conditions of $0 < I_1, I_2 < 1$ or $0 < I_1, I_2 < \min\left\{\frac{\phi}{\alpha-\rho}, 1\right\}$, based on the image of function f. In terms of Eq. (A3), we get the function value of end point about interval $[0, 1]$ and $\left[0, \frac{\phi}{\alpha-\rho}\right]$, i.e.,

$$\begin{aligned} &f(0) = c_1 = -\phi\beta_1\langle k_1\rangle(1-R_0)/R_0, \\ &f(1) = a_1 + b_1 + c_1 = -\alpha(\beta_1\langle k_1\rangle + \beta_2\langle k_2\rangle) - (\gamma+\alpha)(\phi+\rho) < 0, \\ &f\left(\frac{\phi}{\alpha-\rho}\right) = a_1\left(\frac{\phi}{\alpha-\rho}\right)^2 + b_1\frac{\phi}{\alpha-\rho} + c_1 \\ &\quad = -\frac{\beta_2\langle k_2\rangle\phi^3}{(\alpha-\rho)^2} - \frac{\rho\beta_2\langle k_2\rangle\phi^2}{(\alpha-\rho)^2} - \frac{\beta_1\langle k_1\rangle\phi^2}{\alpha-\rho} \\ &\quad\quad - \frac{\rho\beta_1\langle k_1\rangle\phi}{\alpha-\rho} - (\gamma+\alpha)(\phi+\rho). \end{aligned} \tag{A7}$$

If $\alpha > \rho, f(I) = 0$ has one positive root $I_1 \in \left(0, \min\left\{\frac{\phi}{\alpha-\rho}, 1\right\}\right)$ when $f(0) > 0$ $(R_0 > 1)$; $f(I) = 0$ has two positive roots I_1, $I_2 \in \left(0, \min\left\{\frac{\phi}{\alpha-\rho}, 1\right\}\right)$ when $f(0) < 0$, $\Delta_1 > 0$ and $0 < -\frac{b_1}{2a_1} < \min\left\{\frac{\phi}{\alpha-\rho}, 1\right\}$ $\left(R_1^* < R_0 < 1 \text{ and } 1 < R_1 < \min\left\{\frac{2\beta_2\langle k_2\rangle}{\beta_1\langle k_1\rangle} + 1, \frac{2\phi\beta_2\langle k_2\rangle}{(\alpha-\rho)\beta_1\langle k_1\rangle} + 1\right\}, \text{ where } R_1^* = \frac{4\phi(\phi+\alpha)\beta_1\beta_2\langle k_1\rangle\langle k_2\rangle}{(\phi\beta_2\langle k_2\rangle + (\phi+\alpha)\beta_1\langle k_1\rangle)^2}\right)$. If $\alpha < \rho$, $f(I) = 0$ has one positive root $I_1 \in (0, 1)$ when $f(0) > 0$ $(R_0 > 1)$; $f(I) = 0$ has two positive roots $I_1, I_2 \in (0, 1)$ when $f(0) < 0$, $\Delta_1 > 0$ and $0 < -\frac{b_1}{2a_1} < 1$ $\left(R_1^* < R_0 < 1 \text{ and } 1 < R_1 < \frac{2\beta_2\langle k_2\rangle}{\beta_1\langle k_1\rangle} + 1\right)$. Based on the above discussion, we obtain Theorem 1.

2. Stability of equilibria

In this subsection, the dynamics of system (5) in the neighborhood of each equilibrium is investigated.

First, we analyze the stability of the disease-free equilibrium F_0. The Jacobian matrix of system (5) at the disease-free equilibrium F_0 is

$$J_{F_0} = \begin{pmatrix} -(\phi+\rho) & \alpha-\rho \\ 0 & \frac{\phi}{\phi+\rho}\beta_1\langle k_1\rangle - \gamma - \alpha \end{pmatrix}, \tag{A8}$$

and the eigenvalues of J_{F_0} are $\lambda^1_{J_{F_0}} = -(\phi+\rho) < 0$ and $\lambda^2_{J_{F_0}} = \frac{\phi}{\phi+\rho}\beta_1\langle k_1\rangle - \gamma - \alpha$. If $\beta_1 < \beta_1^c$, $\lambda^2_{J_{F_0}} < 0$ and then the disease-free equilibrium F_0 is locally asymptotically stable. When $\beta_1 > \beta_1^c$, $\lambda^2_{J_{F_0}} > 0$ and then F_0 is unstable. Theorem 2 can be proven according to the above analysis.

Then, we study the stability of the endemic equilibria F_1 and F_2. The Jacobian matrix of system (5) at F_1 is

$$J_{F_1} = \begin{pmatrix} -(\phi+\rho) & \alpha-\rho \\ -\beta_1\langle k_1\rangle I_1 - \beta_2\langle k_2\rangle I_1^2 & \Xi_1 \end{pmatrix}, \tag{A9}$$

where $\Xi_1 = (\beta_1\langle k_1\rangle - \gamma - \alpha) - \beta_1\langle k_1\rangle E_1 - 2\beta_2\langle k_2\rangle E_1 I_1 + 2(\beta_2\langle k_2\rangle - \beta_1\langle k_1\rangle)I_1 - 3\beta_2\langle k_2\rangle I_1^2$. Let $g(z) = a_2 z^2 + b_2 z + c_2$, where

$$\begin{aligned} a_2 &= -\frac{3\phi+2\alpha+\rho}{\phi+\rho}\beta_2\langle k_2\rangle, \\ b_2 &= \frac{2\phi}{\phi+\rho}\beta_2\langle k_2\rangle - \frac{2\phi+\alpha+\rho}{\phi+\rho}\beta_1\langle k_1\rangle, \\ c_2 &= \frac{\phi}{\phi+\rho}\beta_1\langle k_1\rangle - (\phi+\rho) - (\gamma+\alpha). \end{aligned} \tag{A10}$$

It is easy to obtain the characteristic polynomial of J_{F_1}

$$\mathscr{P}_{J_{F_1}}(x) = x^2 - tr(J_{F_1})x + \det(J_{F_1}), \tag{A11}$$

where

$$\begin{aligned} \det(J_{F_1}) &= -\phi\beta_1\langle k_1\rangle + (\phi+\rho)(\gamma+\alpha) \\ &\quad + [2(\phi+\alpha)\beta_1\langle k_1\rangle - 2\phi\beta_2\langle k_2\rangle]I_1 \\ &\quad + 3(\phi+\alpha)\beta_2\langle k_2\rangle I_1^2 = \sqrt{\Delta_1}I_1 > 0, \\ \mathrm{tr}(J_{F_1}) &= g(I_1). \end{aligned} \tag{A12}$$

The endemic equilibrium F_1 is locally asymptotically stable only if $tr(J_{F_1}) < 0$, and then we analyze the cases of $tr(J_{F_1}) < 0$, i.e., $g(I_1) < 0$. We further discuss function $g(z)$ to get the explicit conditions of $tr(J_{F_1}) < 0$.

The discriminant of the roots for $g(z) = 0$ is

$$\begin{aligned} \Delta_2 &= \left(\frac{2\phi}{(\phi+\rho)}\beta_2\langle k_2\rangle - \frac{(\alpha+2\phi+\rho)}{(\phi+\rho)}\beta_1\langle k_1\rangle\right)^2 \\ &\quad - \frac{4\phi(3\phi+2\alpha+\rho)\beta_1\beta_2\langle k_1\rangle\langle k_2\rangle}{(\phi+\rho)^2}(1-R_2)/R_2. \end{aligned} \tag{A13}$$

When $\Delta_2 > 0$, we obtain solutions of $g(z) = 0$,

$$\begin{aligned} z_1 &= \frac{2\phi\beta_2\langle k_2\rangle - (\alpha+2\phi+\rho)\beta_1\langle k_1\rangle + (\phi+\rho)\sqrt{\Delta_2}}{2(2\alpha+3\phi+\rho)\beta_2\langle k_2\rangle}, \\ z_2 &= \frac{2\phi\beta_2\langle k_2\rangle - (\alpha+2\phi+\rho)\beta_1\langle k_1\rangle - (\phi+\rho)\sqrt{\Delta_2}}{2(2\alpha+3\phi+\rho)\beta_2\langle k_2\rangle}, \end{aligned} \tag{A14}$$

where $R_2 = \frac{\phi\beta_1\langle k_1\rangle}{(\phi+\rho+\gamma+\alpha)(\phi+\rho)}$. Then, we analyze $g(z) < 0$ under $z \in (0,1)$. We get the function value of end point about interval $[0,1]$, i.e.,

$$\begin{aligned} g(0) &= c_2, \\ g(1) &= -\frac{\phi+2\alpha+\rho}{\phi+\rho}\beta_2\langle k_2\rangle - \frac{\phi+\alpha+\rho}{\phi+\rho}\beta_1\langle k_1\rangle \\ &\quad - (\phi+\rho+\gamma+\alpha) < 0. \end{aligned} \tag{A15}$$

The axis of symmetry of the function $g(z)$ is

$$z^* = 1 - \frac{2\phi+2\alpha+\rho}{3\phi+2\alpha+\rho} - \frac{(2\phi+\alpha+\rho)\beta_1\langle k_1\rangle}{2(3\phi+2\alpha+\rho)\beta_2\langle k_2\rangle} < 1. \tag{A16}$$

When $\Delta_2 < 0$, then $tr(J_{F_1}) < 0$ and F_1 is locally asymptotically stable. If $\Delta_2 > 0$, $g(0) < 0$, and $z^* < 0$ $\left(\text{i.e., } \Delta_2 > 0, \frac{2\phi\beta_2\langle k_2\rangle}{(\alpha+2\phi+\rho)\langle k_1\rangle} < \beta_1 < \frac{(\phi+\rho)(\alpha+\gamma+\phi+\rho)}{\phi\langle k_1\rangle} \text{ and } \beta_2 < \frac{(\phi+\rho)(\alpha+2\phi+\rho)(\alpha+\gamma+\phi+\rho)}{2\phi^2\langle k_2\rangle}\right)$, then $z_2 < z_1 < 0$ and $tr(J_{F_1}) < 0$. If $\Delta_2 > 0$ and $g(0) > 0$ $\left(\text{i.e., } \Delta_2 > 0, \beta_1 > \frac{(\phi+\rho)(\alpha+\gamma+\phi+\rho)}{\phi\langle k_1\rangle}\right)$, then $z_1 > 0$, $z_2 < 0$, $tr(J_{F_1}) < 0$ when $I_1 \in (z_1, 1]$ and $tr(J_{F_1}) > 0$ when $I_1 \in [0, z_1)$. If $\Delta_2 > 0$, $g(0) < 0$ and $z^* > 0$ $\left(\text{i.e., } \Delta_2 > 0, \beta_1 < \min\left\{\frac{(\phi+\rho)(\alpha+\gamma+\phi+\rho)}{\phi\langle k_1\rangle}, \frac{2\phi\beta_2\langle k_2\rangle}{(\alpha+2\phi+\rho)\langle k_1\rangle}\right\}\right)$, then $0 < z_2 < z_1 < 1$ and $tr(J_{F_1}) < 0$ when $I_1 \in [0, z_2) \cup (z_1, 1]$ and $tr(J_{F_1}) > 0$ when $I_1 \in (z_2, z_1)$.

The Jacobian matrix of Eq. (5) at F_2 is

$$J_{F_2} = \begin{pmatrix} -(\phi+\rho) & \alpha-\rho \\ -\beta_1\langle k_1\rangle I_2 - \beta_2\langle k_2\rangle I_2^2 & \Xi_2 \end{pmatrix}, \tag{A17}$$

where $\Xi_2 = (\beta_1\langle k_1\rangle - \gamma - \alpha) - \beta_1\langle k_1\rangle E_2 - 2\beta_2\langle k_2\rangle E_2 I_2 + 2(\beta_2\langle k_2\rangle - \beta_1\langle k_1\rangle)I_2 - 3\beta_2\langle k_2\rangle I_2^2$. We calculate

$$\begin{aligned} \det(J_{F_2}) &= \phi\beta_1\langle k_1\rangle + (\phi+\rho)(\gamma+\alpha) \\ &\quad + [2(\phi+\alpha)\beta_1\langle k_1\rangle - 2\phi\beta_2\langle k_2\rangle]I_2 + 3(\phi+\alpha)\beta_2\langle k_2\rangle I_2^2 \\ &= -\sqrt{\Delta_1}I_2 < 0, \end{aligned} \tag{A18}$$

and then J_{F_2} has a positive eigenvalue and a negative eigenvalue. Hence, the endemic equilibrium F_2 is a saddle. Based on the above analysis, we can get Theorem 3.

REFERENCES

[1] R. Pastor-Satorras and A. Vespignani, "Epidemic spreading in scale-free networks," Phys. Rev. Lett. **86**, 3200–3203 (2001).
[2] M. E. J. Newman, "Spread of epidemic disease on networks," Phys. Rev. E **66**, 016128 (2002).
[3] R. Pastor-Satorras, C. Castellano, P. Van Mieghem, and A. Vespignani, "Epidemic processes in complex networks," Rev. Mod. Phys. **87**, 925–979 (2015).
[4] C. C. McCluskey, "Complete global stability for an SIR epidemic model with delay-distributed or discrete," Nonlinear Anal.-Real World Appl. **11**, 55–59 (2010).
[5] B. M. Behring, A. Rizzo, and M. Porfiri, "How adherence to public health measures shapes epidemic spreading: A temporal network model," Chaos **31**, 043115 (2021).
[6] J. X. Yang, "Epidemic spreading on multilayer homogeneous evolving networks," Chaos **29**, 103146 (2019).
[7] G. Zaman, Y. H. Kang, and I. H. Jung, "Stability analysis and optimal vaccination of an SIR epidemic model," BioSystems **93**, 240–249 (2008).
[8] A. Gray, D. Greenhalgh, L. Hu, X. Mao, and J. Pan, "A stochastic differential equation SIS epidemic model," SIAM. J. Appl. Math. **71**, 876–902 (2011).
[9] L. J. S. Allen and A. M. Burgin, "Comparison of deterministic and stochastic SIS and SIR models in discrete time," Math. Biosci. **163**, 1–33 (2000).
[10] Z. Q. Li, P. C. Zhu, D. W. Zhao, Z. H. Deng, and Z. Wang, "Suppression of epidemic spreading process on multiplex networks via active immunization," Chaos **29**, 073111 (2019).
[11] G. F. de Arruda, G. Petri, and Y. Moreno, "Social contagion models on hypergraphs," Phys. Rev. Res. **2**, 023032 (2021).

[12]N. W. Landry and J. G. Restrepo, "The effect of heterogeneity on hypergraph contagion models," Chaos **30**, 103117 (2020).
[13]G. Ferraz de Arruda, M. Tizzani, and Y. Moreno, "Phase transitions and stability of dynamical processes on hypergraphs," Commun. Phys. **4**, 1–9 (2021).
[14]I. Iacopini, G. Petri, A. Barrat, and V. Latora, "Simplicial models of social contagion," Nat. Commun. **10**, 2485 (2019).
[15]J. Matamalas, S. Gomez, and A. Arenas, "Abrupt phase transition of epidemic spreading in simplicial complexes," Phys. Rev. Res. **2**, 012049 (2020).
[16]D. Wang, Y. Zhao, J. F. Luo, and H. Leng, "Simplicial SIRS epidemic models with nonlinear incidence rates," Chaos **31**, 053112 (2021).
[17]P. Cisneros-Velarde and F. Bullo, "Multi-group SIS epidemics with simplicial and higher-order interactions," IEEE Trans. Control Netw. Syst. **9**, 695–705 (2021).
[18]J. Liu, Y. Tang, and Z. Yang, "The spread of disease with birth and death on networks," J. Stat. Mech.: Theory Exp. **8**, P08008 (2004).
[19]J. Zhang and Z. Jin, "The analysis of an epidemic model on networks," Appl. Math. Comput. **217**, 7053–7064 (2011).
[20]X. Wei, G. Xu, L. Liu, and W. Zhou, "Global stability of endemic equilibrium of an epidemic model with birth and death on complex networks," Phys. A **477**, 78-84 (2017).
[21]A. L. Barabási and R. Albert, "Emergence of scaling in random networks," Science **286**, 509–512 (1999).
[22]M. E. J. Newman, "Finding community structure in networks using the eigenvectors of matrices," Phys. Rev. E **74**, 036104 (2006).
[23]D. E. Knuth, *The Stanford GraphBase: A Platform for Combinatorial Computing* (ACM Press, New York, 1993).
[24]M. Martcheva, *An Introduction to Mathematical Epidemiology* (Springer, 2010).
[25]D. M. Bortz and P. W. Nelson, "Sensitivity analysis of a nonlinear lumped parameter model of HIV infection dynamics," Bull. Math. Biol. **66**, 1009–1026 (2004).